

UNCLASSIFIED

AD NUMBER
AD463881
NEW LIMITATION CHANGE
TO Approved for public release, distribution unlimited
FROM Distribution authorized to U.S. Gov't. agencies and their contractors; Administrative/Operational Use; APR 1965. Other requests shall be referred to Office of Naval Research, One Liberty Center, 875 North Randolph Street, Arlington, VA 22203-1995.
AUTHORITY
onr memo, 28 dec 1965

THIS PAGE IS UNCLASSIFIED

UNCLASSIFIED

AD 4 6 3 8 8 1

DEFENSE DOCUMENTATION CENTER

FOR

SCIENTIFIC AND TECHNICAL INFORMATION

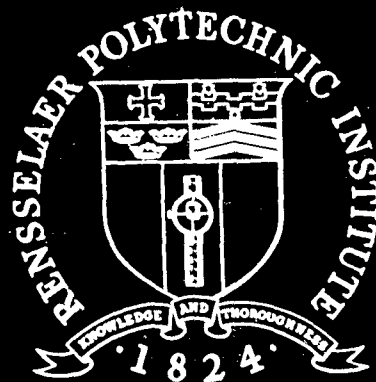
CAMERON STATION ALEXANDRIA, VIRGINIA



UNCLASSIFIED

NOTICE: When government or other drawings, specifications or other data are used for any purpose other than in connection with a definitely related government procurement operation, the U. S. Government thereby incurs no responsibility, nor any obligation whatsoever; and the fact that the Government may have formulated, furnished, or in any way supplied the said drawings, specifications, or other data is not to be regarded by implication or otherwise as in any manner licensing the holder or any other person or corporation, or conveying any rights or permission to manufacture, use or sell any patented invention that may in any way be related thereto.

4 6 3 8 8 1



**Rensselaer Polytechnic Institute**

**Troy, New York**

AVAILABLE COPY WILL NOT PERMIT  
FULLY LEGIBLE REPRODUCTION  
REPRODUCTION WILL BE MADE IF  
REQUESTED BY USERS OF DDC.

OFFICE OF NAVAL RESEARCH

Contract Nonr-591 (19)

Task No. NR 051-428

Technical Report No. 8

Extended Chain Polymer Crystals

by

Tamio Arakawa

JUN 2 1965  
LIBRARY V 511  
ASA 2

A Thesis

Presented to the Faculty of the Graduate School  
of Cornell University for the Degree  
of Doctor of Philosophy in  
November, 1964, under the  
Direction of Bernhard Wunderlich  
Assoc. Prof. of Chemistry, Dept. of Chemistry  
Rensselaer Polytechnic Institute

Parts of this thesis have been published in the Journal of  
Polymer Science (Vol. 2A, 3697-3707, 1964) and will be presented at the  
IUPAC Polymer Meeting in Prague, September, 1965, to be printed in J.  
Polymer Sci., Part C.

(Reproduction in whole or part is permitted for any  
purpose of the United States Government.)

April, 1965

## ACKNOWLEDGMENTS

The author wishes to express his most sincere appreciation to Professor Bernhard Wunderlich for his advice and guidance throughout this research. He also wishes to thank Professor Franklin A. Long, Professor Benjamin Widon and Professor Robert H. Silsbee for serving on his committee. The criticism and suggests for the thesis which were received from Professor Robert E. Hughes are gratefully acknowledged. Appreciation is also extended to Professor Philip H. Geil of the Case Institute of Technology and to Dr. Franklin R. Anderson of Chemstrand Research Center, to whom the author owes most of the electron microscopy and small angle x-ray studies.

The financial support of the Advanced Research Projects Agency through the Materials Science Center of Cornell University and of the Office of Naval Research is gratefully acknowledged. A Fulbright Travel Grant, the Sprague Electric Company Fellowship and the Eastman Kodak Scientific Award were also invaluable to the author. The author also thanks Teijin, Ltd., of Tokyo, Japan, for granting him a leave of absence for the completion of his graduate studies.

The assistance of Mrs. Betty Blake, Mrs. Barbara Boettcher, Mrs. Ruth Snyder and Miss Elise Armistead of the Materials Science Center in preparing the manuscript is very much appreciated.

Finally the author wishes to thank his wife, Katsu, for her help and encouragement throughout the course of his studies at Cornell.

## TABLE OF CONTENTS

<u>Chapter</u>		<u>Page</u>
I	INTRODUCTION . . . . .	1
II	EXPERIMENTAL . . . . .	6
	A. Pressurestat and Crystallization Procedure . . . . .	6
	B. Differential Thermal Analysis (DTA). . . . .	13
	C. Density Determination . . . . .	15
	D. Dilatometry . . . . .	16
	E. X-ray Diffraction (Wide Angle) . . . . .	19
	F. Small Angle X-ray Scattering and Electron Microscopy . . . . .	20
	G. Calorimetry . . . . .	20
	H. Materials . . . . .	21
III	RESULTS . . . . .	27
	A. Linear Polyethylene . . . . .	27
	a) DTA, Density and Wide Angle X-ray Diffraction . . . . .	27
	b) Electron Microscopy and Low Angle X-ray Diffraction . . . . .	34
	B. Polymethylene and Polyethylene Copolymers . . . . .	41
	a) DTA, Density, Dilatometry, and Calorimetry . . . . .	41
	b) Electron Microscopy . . . . .	46

<u>Chapter</u>		<u>Page</u>
IV	DISCUSSION . . . . .	61
	A. Morphology . . . . .	61
	B. Behavior of Polymers under Pressure. .	67
	C. Crystallization of Linear Polyethylenes at High Pressure . . . . .	71
	D. Melting of Polyethylenes and Poly- methylene with Extended Chain Structure . . . . .	78
	E. Melting of Polyethylene Copolymers with Extended Chain Structure . . . . .	86
	REFERENCES . . . . .	96

## LIST OF TABLES

<u>Table</u>		<u>Page</u>
1	Calibration of Pressure Recording . . . . .	9
2	Molecular Weight of Polyethylenes . . . . .	24
3	Properties of Ethylene-butene-1 Copolymers . . . . .	26
4	Description of Ethylene-propylene Copolymers. . . . .	26
5	Data of Polyethylene Crystallized under Different Pressures . . . . .	28,29
6	Small Angle Diffraction . . . . .	38
7	Data of Polymethylene, Polyethylenes and Poly- ethylene Copolymers Crystallized at High Pressure . . . . .	42,43
8	Dependence of the Density of Marlex 50 on Crystallization Temperature at a Constant Crystallization Pressure of 4,300atm . . . . .	44
9-17	Dilatometry of Samples 31-39 . . . . .	47-55
18	Specific Volume of Polyethylene . . . . .	68
19	Surface Free Energy of Polyethylene Lamellae Crystallized from Melt and Solution . . . . .	86

## LIST OF ILLUSTRATIONS

<u>Figure</u>		<u>Page</u>
1	Schematic diagram of high pressure system . .	7
2	Electrical circuit diagram of pressurestat .	10
3	Sample container for crystallization at high pressure . . . . .	12
4	Cumulative molecular length distribution of polyethylenes . . . . .	23
5	Cumulative molecular length distribution of ethylene-butene-1 copolymers . . . . .	25
6	DTA traces of polyethylene samples crystal- lized under elevated pressure . . . . .	31
7	DTA traces of polyethylene crystallized at high pressure . . . . .	32
8	Stepwise DTA of sample 15 . . . . .	33
9	Experimental maximum melting points of pressure-crystallized polyethylene . . . .	35
10	Density of polyethylene crystallized under elevated pressure . . . . .	36
11	Relation between x-ray crystallinity and density crystallinity . . . . .	37
12	Electron micrographs and selected area dif- fraction pattern of pressure-crystallized polyethylene . . . . .	39
13	DTA traces of polyethylene copolymers crystallized at high pressure . . . . .	45
14	Superheating of extended chain crystals . . .	56
15	Melting curves of polymethylene and poly- ethylene . . . . .	57

<u>Figure</u>		<u>Page</u>
16	Melting curves of ethylene-butene-1 copolymers . . . . .	58
17	Melting curves of ethylene-propylene copolymers . . . . .	59
18	Electron micrographs of fracture surfaces of pressure-crystallized polymethylene . . . .	60
19	Crystallinity by density of polyethylene copolymers crystallized at high pressure .	89
20	Melting points of polyethylene copolymers crystallized at high pressure . . . . .	91

## ABSTRACT

Linear polyethylene has been crystallized from the melt under pressure up to 5300atm and at temperatures up to 236°C. A specially designed pressurestat was used, which could maintain constant elevated hydrostatic pressure up to 6500atm for long periods of time. Crystallization conditions of constant supercooling and constant cooling rates were employed.

Electron micrographs of fracture surfaces obtained from these pressure-crystallized samples show that the formation of extended chain lamellae is the dominant mode of crystallization when high crystallization pressure ( $> 3500\text{atm}$ ) and temperature ( $> 170^\circ\text{C}$ ) are employed. Extended chain lamellae as thick as  $3\mu$  were observed. The chains were found to be oriented perpendicular to the surfaces of lamellae.

DTA of the samples has shown that the polymer molecules crystallize primarily in the form of folded chain lamellae at crystallization pressures up to 2000atm, their melting points becoming higher with increasing pressure. At pressures ranging from 2000atm to 3500atm, folded chain lamellae gradually give way to extended chain lamellae. The high temperature peak, which first appears in this pressure range, reaches a plateau of  $140^\circ\text{C}$  at 4000atm. Small low temperature peaks, which always accompany the high temperature peak of

pressure-crystallized unfractionated polyethylene, were attributed to the low molecular weight fraction in the polymer. It was concluded that the formation of extended chain lamellae is a rapid process at appropriate pressures and temperatures, pressure being the more important factor.

The crystallinity of pressure-crystallized polyethylene samples was determined both by density measurement and by x-ray diffraction. A good agreement was obtained between the two procedures. Density as high as 0.997g/ml at 25°C was achieved. X-ray diffraction showed no irreversible change of the orthorhombic unit cell of polyethylene by pressure.

Polymethylene (M.W. ca.  $10^7$ ), ethylene-butene-1 copolymers, and ethylene-propylene copolymers were also crystallized at high pressure. The samples were studied by means of DTA, density measurement, calorimetry and dilatometry. It has been observed that dilatometry gives considerably lower melting points for these samples compared with the DTA, and that the DTA peak temperatures of the samples are strongly dependent on the heating rate. Superheating of the thick lamellae was proven to be the case.

Electron micrographs of the fracture surfaces of pressure-crystallized polymethylene show that the lamellae in this sample are as thick as  $6\mu$ . As the polymer contains neither low molecular weight fraction nor enough side chains to

cause an appreciable melting point depression, its dilatometric melting point of  $141.4^{\circ}\text{C}$  has been identified as  $T_m^{\circ}$ , the equilibrium melting point of the linear polyethylene with infinite molecular weight.

Combining the experimental  $T_m^{\circ}$  with peak temperatures and low angle x-ray data, a surface energy of  $90 \text{ erg/cm}^2$  was calculated for low and atmospheric pressure-crystallized lamellae of linear polyethylene.

Introduction of methyl and ethyl side chains up to two per 100 chain carbon atoms was observed to reduce the crystallinity of the pressure-crystallized polyethylene. However, the dilatometric melting point was observed to remain unchanged. It has been proposed that these side chains can be accommodated in the crystal lattice of polyethylene.

The formation of extended chain crystals appears to be hindered by the introduction of side chains through their effect on the bulk viscosity of the samples at high pressure.

## I. INTRODUCTION

The solid state of linear high polymers has been a primary interest throughout the history of polymer science.

Prior to general acceptance that polymers are very long chain molecules, the application of x-ray diffraction showed that many polymers, natural and synthetic, contained crystalline regions.<sup>1</sup> The unit cell dimensions were found to be similar in size to those of low molecular weight compounds. The Bragg reflections, however, were less sharply defined and were often accompanied by a broad diffuse background. The diffuseness of the diffraction patterns was attributed to the dimensions of the crystallites in polymers. Thus the size of the crystallites was estimated from the x-ray line broadening, by the use of Scherrer's equation,<sup>2</sup> to be a few hundred Angstroms for most polymers. The broad diffuse background was accepted as due to liquid-like or amorphous structure in polymeric materials.

Recognition of the unusually high molecular weight of polymers, coupled with the crystallites' size of a few hundred Angstroms, led to the concept of the "fringed micelle" structure of semicrystalline linear polymers.<sup>3</sup> In this model a polymer chain, which may be typically 10,000 to 100,000A long, is visualized as going through various crystalline and amorphous regions. The identity of a long molecule has been assumed, in this case, to be obscured, and a

one component, two-phase treatment of a semicrystalline polymer, disregarding the molecular weight distribution, may be satisfied approximately. Thermodynamic arguments based on the "fringed micelle" two-phase model made a considerable contribution to the elucidation of equilibrium phenomena in the bulk state of polymers.<sup>4</sup>

Although the fringed micelle model could give satisfactory explanations to various experimental observations, its statistical nature of accommodating polymer molecules into crystalline and amorphous regions made it difficult to explain the development of the spherulite, which is a dominant morphological feature of bulk crystallized homopolymers.

The discovery of solution-grown thin lamellar single crystals of linear polyethylenes in 1957 has opened a new phase of the study of solid state polymers.<sup>5-7</sup> These lamellar single crystals have been shown to be about 100A thick. The polymer chains are oriented perpendicular to the lamella and fold back and forth on themselves regularly at the surface of the lamella. Further study has revealed that almost all crystalline linear polymers can be crystallized as the folded chain lamellar single crystals from dilute solutions.<sup>8</sup> Single crystals with similar structures were also observed in some linear polymers crystallized from the melt.<sup>7-11</sup> Furthermore, electron microscopic observations have revealed that the complex organization of spherulites consists of lamellar

structures for almost all the polymers studied.<sup>8</sup> Thus the view is becoming increasingly accepted that "all crystalline polymers can and usually do crystallize from the melt and from solution in the form of thin lamellae, on the order of one to several hundred Angstroms thick, in which the molecules are folded."<sup>8</sup>

However, it is clear that even a perfect lamellar single crystal with chain foldings cannot be the thermodynamically most stable crystal structure. For linear polyethylene and for many polymers with similar molecular structures, the stable crystal morphology should rather be a crystal composed of fully extended molecules with the planar zigzag conformation, since the energy of the trans conformation is less than that of the gauche conformation.<sup>12</sup> Experimentally, this is supported by the fact that lamellae can easily be thickened by heat treatment, but never be made thinner.<sup>8</sup> Thus a lamellar structure in polymer crystallization is a compromise between thermodynamic and kinetic effects in the process of crystallization.

The growth of extended chain crystals, which are of fundamental importance for the thermodynamic treatment of the equilibrium phenomena in polymers, has been a major unsolved problem. One attack on the problem has been to crystallize polymers from the melt with possible minimum supercooling.

Crystallization of linear polyethylene by Mandelkern and co-workers,<sup>13</sup> and by Flory and co-workers,<sup>14</sup> in which a small degree of supercooling coupled with tediously long crystallization time was used, has raised the low angle x-ray spacing, and probably the fold length, to about 1,000A. Because the rate of nucleation and the rate of crystal growth decrease rapidly with decreasing degree of supercooling, it will be practically impossible to make the thickness of lamellae much higher than the above value by employing higher crystallization temperature.

The phase rule tells us that the limitation in the crystallization temperature can only be avoided by raising the crystallization pressure. The crystallization and melting under elevated pressure were carried out for some linear polymers<sup>15</sup> including polyethylene<sup>16-21</sup> mainly to obtain information on their phase diagrams and thermodynamic quantities. However, it is expected that the morphology of solid state polymers can also be altered by the application of high pressure during the crystallization.

In this thesis I am going to discuss the effect of high crystallization pressure on the morphology of polymethylene, linear polyethylene, and some polyethylene copolymers. The properties of the solid state polymers thus crystallized will also be described. Among other results it will be shown that:

- a) Polymethylene, linear polyethylene, and polyethylene copolymers with methyl or ethyl side groups (up to two per one hundred chain carbon atoms) can be crystallized in the form of very thick lamellae in which the effect of surface energy is negligibly small.
- b) In these lamellae, molecular chains are fully extended.
- c) The equilibrium melting point of an infinite molecular weight linear polyethylene is  $141.4^{\circ}\text{C}$ .
- c) The extended chain lamellae can easily be superheated in the process of melting.
- e) The melting point of an extended chain lamella of linear polyethylene is not depressed by the introduction of methyl or ethyl side chains up to two per one hundred chain carbon atoms.
- f) The formation of extended chain lamellae is hindered by the introduction of side chains.

These experiments show for the first time conclusively that the folded chain conformation in crystalline polymers can be avoided and that equilibrium crystals can be grown.

## II. EXPERIMENTAL

### A. Pressurestat and Crystallization Procedure<sup>22</sup>

The schematic diagram of the pressurestat used for the crystallization of samples is shown in Fig. 1. The high pressure vessel in which crystallizations were performed is constructed as a two-ended cylinder. The closures employ Bridgman seals.<sup>23</sup> The internal cavity dimensions are 1.5" diameter and 7" length. The hydrostatic pressure line is connected to the bottom, while the top closure has been used to load the samples into the cavity. The high pressure cylinder is removed from the pressure line by uncoupling a straight-through connector.

The pressure vessel assembly is immersed in a 55gal constant temperature oil bath. The bath contains four heaters with the following wattages: 250, 300, 750, and 1,000. Hydrocarbon oil is usable for operation up to 170°C. The temperature of the oil bath could be controlled to  $\pm 0.1^\circ\text{C}$ . When all heaters are turned off, the temperature of the bath decreases at the rate of 4°C/hour at 170°C, the rate decreasing as the temperature comes closer to room temperature.

For temperatures higher than 170°C, the pressure vessel was directly wrapped with two heating wires which were covered with asbestos tubing. Finally the vessel was covered with one half inch of asbestos. The wattage of the auxiliary

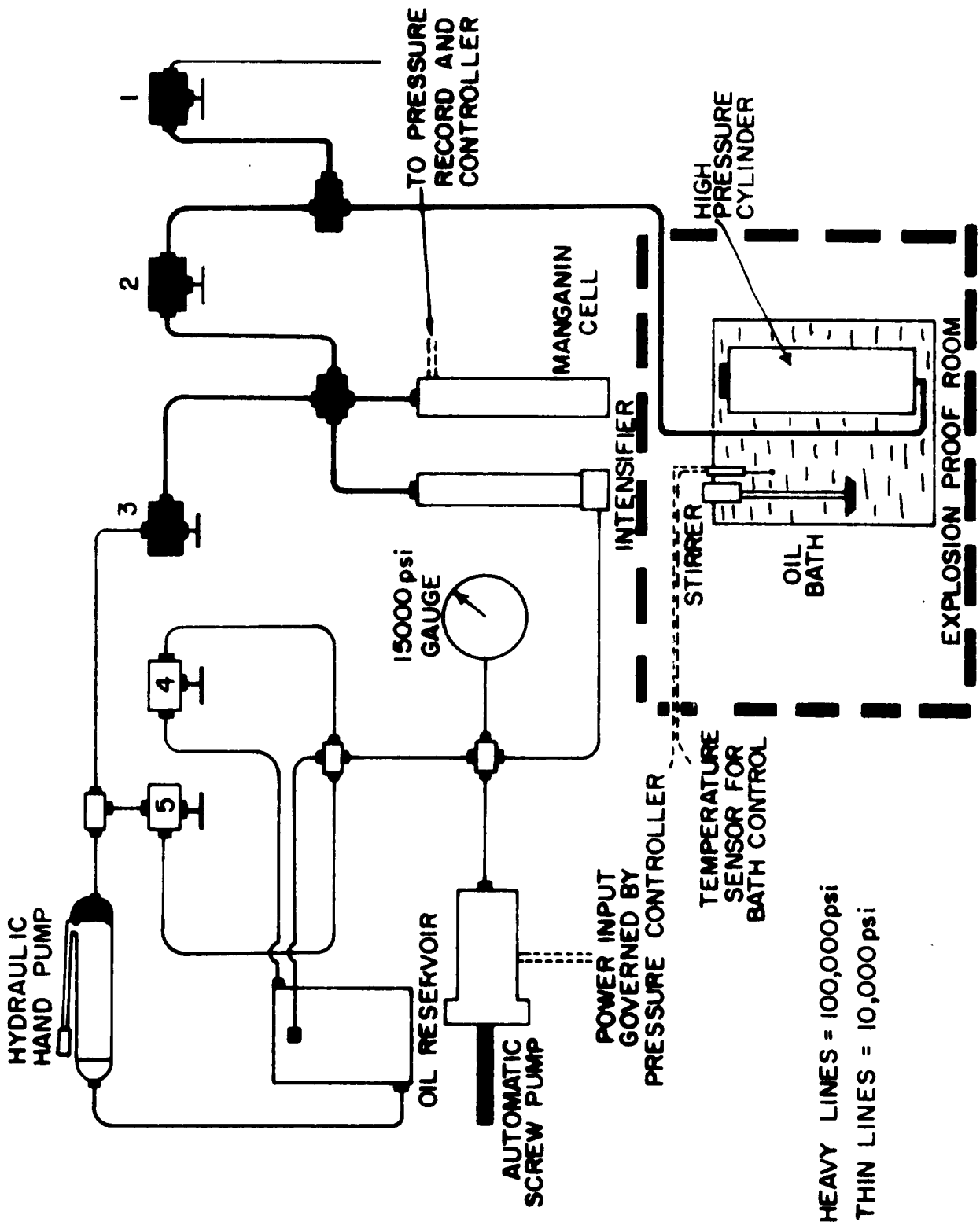


Figure 1. Schematic diagram of high pressure system.

heater was controlled with a variac. The main heater was connected to a F&M model 40 linear temperature programmer, which controlled the temperature of the vessel through an iron-constantan thermocouple placed against the wall of the vessel. The true temperature of the vessel was calibrated by directly measuring the temperature of the hydrocarbon oil inside the bomb with a thermocouple. By this method the temperature was estimated to be controlled within 1°C. The linear temperature programmer was used to cool the vessel at a constant rate down to room temperature. The rate of cooling could be changed from 1°C/hour to 14°C/hour.

A manganin wire cell has been chosen as a pressure sensing device.<sup>24</sup> The resistance changes were recorded by a Dynalog Cell Recorded model 9420T produced by the Foxboro Company. Mechanical high-low contacts kept the pressure within 1% of the full deflection (dead band). The recorder-controller has three ranges: 0 to 1,650atm (scale 1), 0 to 3,300atm (scale 2), and 0 to 6,600atm (scale 3). Internal calibration gave actual factors 3.587 for scale 1 and 1.925 for scale 2 with respect to scale 3.

Calibration of the manganin gauge was done against a rotating piston press using a National Bureau of Standards calibrated proving ring. The final results of the calibration of scale 3 are given in Table I. The accuracy of the pressure recording over the whole range is 1.5%.

TABLE I. CALIBRATION OF PRESSURE RECORDING

<u>Pressure indicated by the recorder</u>	<u>Actual pressure</u>
10,000 psi	9,360 psi
20,000	18,740
30,000	28,760
40,000	38,130
50,000	47,500
60,000	57,150
70,000	66,520
80,000	76,520
90,000	85,570
100,000	95,000

The electrical circuit diagram is given in Fig. 2. The forward and reverse contacts are activated by the respective coils at the bottom of the diagram. The controller transfers the contact signals to a reversible motor-driven screw-type 600atm pump on the low pressure side of the system. The forward or reverse motions of the screw pump keeps the high pressure to the preset value by means of a 1:11.1 ratio intensifier. The manual operation of the hydraulic pump is used for the initial increase of the pressure. For a completely liquid system the pressurization from 0 to 6,600atm could be achieved in 5 minutes.

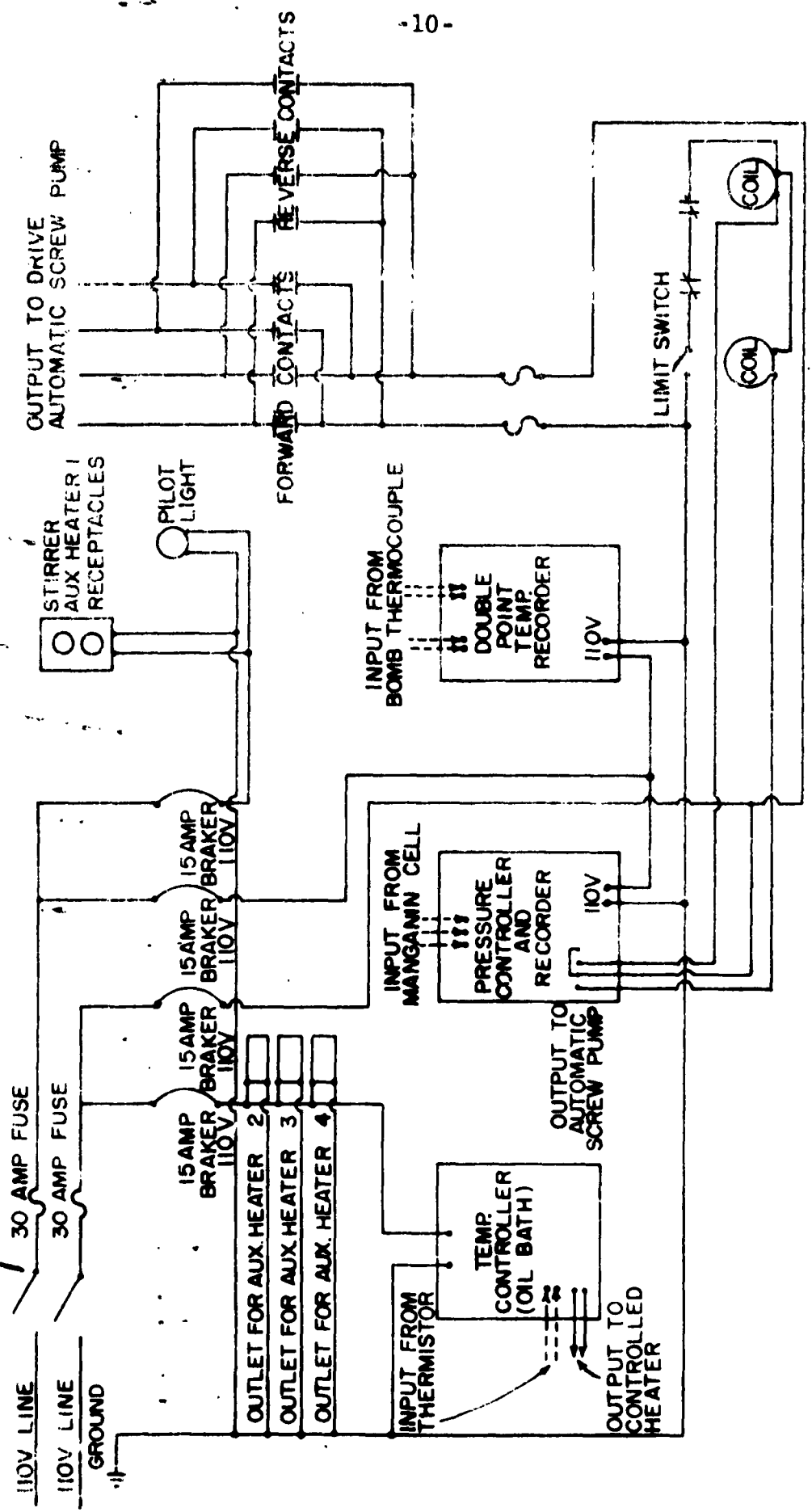


Figure 2. Electrical circuit diagram of pressurostat.

The capacities involved in the pressure apparatus are: 203ml for the high pressure cylinder, 202ml for the screw pump, 161ml for the low pressure chamber of the intensifier, and 14.4ml for the high pressure chamber of the intensifier.

Polymer samples were generally crystallized in oil-tight thin brass bellows such as that shown in Fig. 3. The container consists of brass bellows with an outer diameter of 5/8" and an inner diameter of 3/8", a brass disk bottom, and a brass head which is specially designed to introduce and seal the sample in the container.

The three parts are connected by silver soldering. Before use, the containers were washed with dilute sulfuric acid to remove the oxide film on the surface, washed thoroughly with distilled water and dried. The container was half filled with sample powder or pellets and was then kept in a vacuum oven at 170°C for several hours. By repeating this procedure, the container was finally filled with 5 to 10g of sample up to an inch or two from the top.

After completely replacing the air in the bellows with nitrogen, the top of the container was sealed with metal lead while keeping its main part in the water to avoid the degradation of the sample. Lead was used as sealant because its melting point is not high enough to destroy the sample and it can stand pressure up to at least 240°C, the highest temperature employed in the experiments.

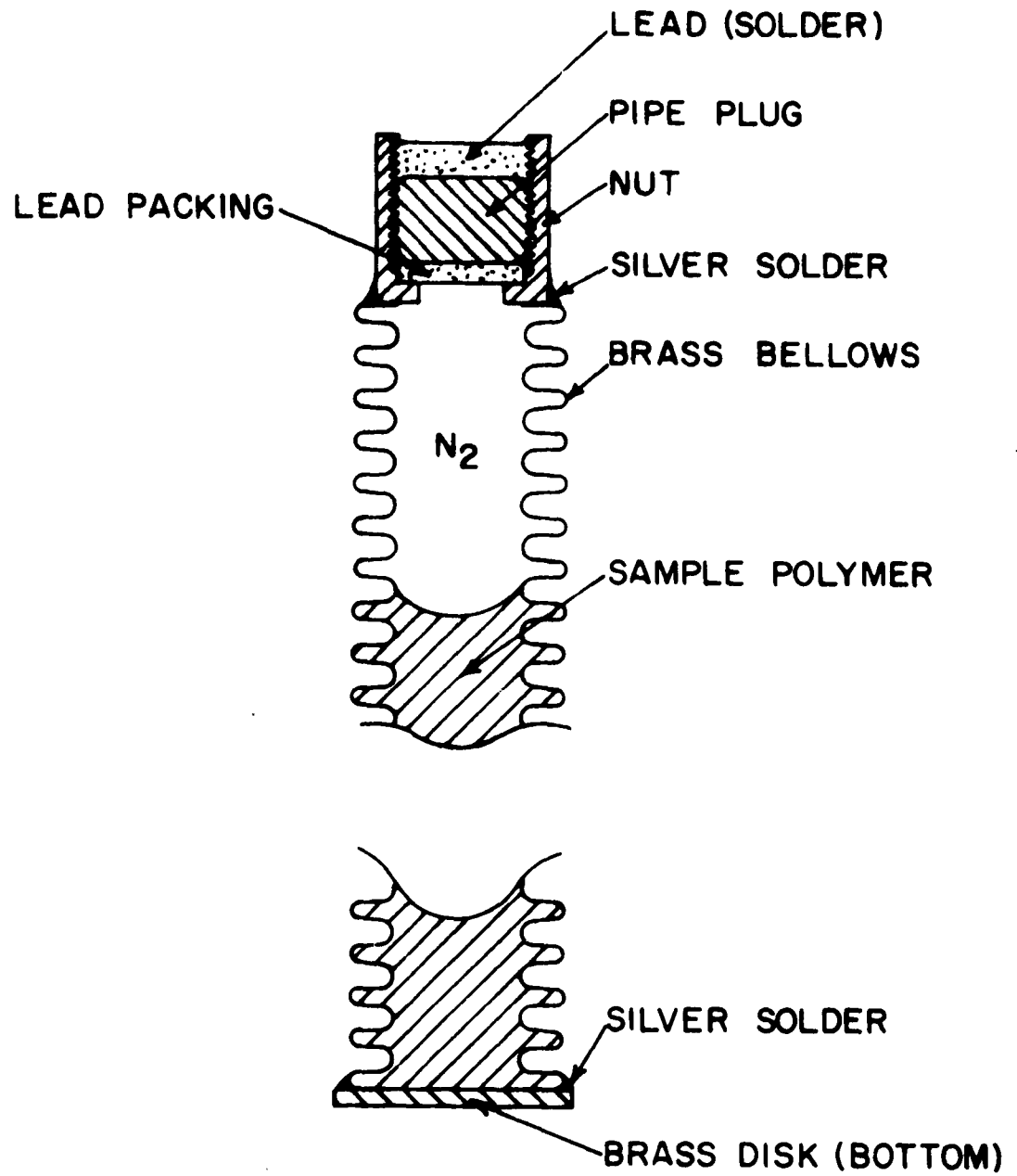


Figure 3. Sample container for crystallization at high pressure.

A typical crystallization procedure is as follows: the bellows containing the sample are put into the pressure bomb. The bomb is filled with hydrocarbon oil, sealed, and connected to the pressure line. After the bomb is heated to the preset temperature, the system is first quickly pressurized with the hand pump, and afterward the pressure control is left to the recorder-controller. For temperatures higher than 170°C, slight pressure (about 2,000 psi) was applied when the temperature reached 170°C in order to avoid thermal decomposition of the oil. The system was kept at these temperatures and pressures for a certain period of time for crystallization. Subsequently, cooling started with a controlled rate, the pressure being kept constant. The pressure was released after the temperature dropped below 50°C and the sample was taken out of the bellows afterwards. All analyses of the sample were carried out at atmospheric pressure.

#### B. Differential Thermal Analysis (DTA)

Two different types of DTA apparatus were used to study the melting properties of the samples. The description of the first apparatus and the determination of melting points from DTA charts are described elsewhere.<sup>25</sup> Theoretical treatment of this type of apparatus was also carried out.<sup>26</sup> The samples were cut out of the original blocks with a lathe

so that they were tightly fitted to the sample holder and the thermocouple sheath. When the sample was very brittle or powdery, it was squeezed into the sample holder with a metal rod, which was tightly fitted to the holder and had an extruding tip at the top which was designed to leave a hole at the center of the sample for the thermocouple. The weight of the sample was controlled to  $0.50 \pm 0.01$ g with few exceptions. It should be noted that the heating rate is not exactly constant, but slowly decreases as the temperature rises, as constant voltage is employed for heating. A typical example is as follows.

<u>Temperative range</u>	<u>Average heating rate</u>
39 - 77°C	2.00°C/min
77 - 113°C	1.64°C/min
113 - 150°C	1.48°C/min

The average heating rate between 77°C and 113°C has been employed as "heating rate" in the following discussions. The beginning of melting was arbitrarily taken at the temperature where the temperature difference recording had deviated from the base line by 5% of the total melting peak height. The maximum melting point is defined as the point where the last detectable amount of heat of fusion is absorbed. The procedure to obtain this point is also described elsewhere.<sup>25</sup>

The iron-constantan thermocouple which was used for measuring the sample temperature had been calibrated against a platinum resistance thermometer. The error of temperature recording was less than 0.1°C.

For some cases, where rapid heating was necessary or when the amount of sample was limited, a commercial du Pont 900 Differential Thermal Analyzer was used. With this apparatus, controlled heating rates ranging from 0.5°C/min to 80°C/min were available. Small amounts of sample mixed with glass powder were heated in a glass tube 2mm in diameter. The analysis of the results is similar to that described for the first apparatus, although the maximum melting point could not be extrapolated for this equipment.

#### C. Density Determination

Density gradient columns consisting of toluene-chlorobenzene mixtures were used. Commercial glass floats with density accurately measured to  $10^{-5}$  g/ml made up the references. By employing small density gradients, the density of the samples could be measured to  $\pm 0.0002$  g/ml. Samples were cut into small pieces (ca.  $1\text{mm}^3$ ). In order to avoid the error caused by the air absorbed by the sample pieces, they were kept in vacuum for half an hour prior to the measurement. They were then immersed in toluene without

breaking the vacuum and were transferred into the column. All measurements were done at 25°C.

The density crystallinities were calculated from the expression

$$C_W = \frac{\bar{V}_a - \bar{V}}{\bar{V}_a - \bar{V}_c} \quad (1)$$

where  $\bar{V}$  is the specific volume of the sample,  $\bar{V}_a$  is the specific volume of the sample when it is completely amorphous, and  $\bar{V}_c$  is the specific volume of the sample when completely crystalline.

For polymethylene, polyethylenes, ethylene-butene copolymers and ethylene-propylene copolymers,  $\bar{V}_c$  at 25°C is given by Swan<sup>27</sup> as 1.001ml/g and 1.173ml/g for  $\bar{V}_a$  at 25°C. This value has been adopted as the average of the values given by Gubler and Kovacs,<sup>28</sup> and Nielsen.<sup>29</sup>

#### D. Dilatometry

The changes in specific volume with temperature were measured with dilatometers. The procedure employed by Bekkedahl<sup>50</sup> and Aggarwal et al.<sup>31</sup> was closely followed. Precision bore tubings with an inside diameter of 1.00±0.01mm produced by Kontes Glass Company were used without calibration. A weighed quantity of sample, usually 0.5 to 1.0g, was cut into small pieces and was sealed in the 13mm diameter pyrex tube which served as the reservoir of the dilatometer.

A hollow pyrex bulb, 30 to 40mm long and 10mm in diameter, was inserted between the sample and the bottom of the reservoir to avoid any thermal effect on the sample on sealing. The sample had been kept in vacuum at 100°C for a few hours before an appropriate amount of instrument grade mercury was introduced into the dilatometer using the technique described by Aggarwal et al.<sup>31</sup>

The effect of trapped air was estimated to be negligible compared to other errors like diameter of precision bore tubes, density of the sample, and so on. The temperature of the oil bath was controlled with thermistors. The temperature of the bath was measured with a thermometer which had been calibrated against a platinum resistance thermometer to 0.05°C. Continuous recording of the bath temperature for four hours showed that the temperature control was better than 0.1°C at 140°C. The change in the height of the mercury in the capillary was followed with a cathetometer. Temperature of the bath was increased step-wise. At each temperature, measurement was carried out after no further change in height was observed within an hour. Generally 12 to 24 hours were spent for each temperature step when melting was going on. The specific volume of the sample was calculated from the density at 25°C, the height of the mercury column, and the thermal expansion of the reservoir.

The degree of crystallinity was calculated from the measured specific volume  $\bar{V}$ , assuming additivity of volume of crystalline and amorphous phases. The weight fraction of the crystalline phase is then given by Eq. (1).

The relation between  $\bar{V}_c$  and temperature  $t$  ( $^{\circ}\text{C}$ ) is given by Flory and co-workers,<sup>32</sup> based on the x-ray unit cell determinations by Cole and Holms<sup>33</sup> and by Swan,<sup>27</sup> as

$$\bar{V}_c = 0.993 + 3.0 \times 10^{-4} t \quad (2)$$

Because of the errors introduced by many factors such as the diameter of the capillaries, their tilting from the vertical position, trapped air, density measurement, etc., the measured specific volumes of the samples above the melting points do not exactly agree among themselves as function of temperature.

As a means of avoiding this difficulty, a correction has been applied to  $\bar{V}_a$  such that  $\bar{V}_a$  is a linear function of  $t$ , and that the amorphous specific volume is 1.173 at  $25^{\circ}\text{C}$ . Then  $\bar{V}_a$  for any sample can be calculated by

$$\bar{V}_a(t) = 1.173 + \left[ \frac{\bar{V}_a(t_0) - 1.173}{t_0 - 25} \right] (t - 25) \quad (3)$$

where  $\bar{V}_a(t_0)$  is a point on the experimentally obtained  $\bar{V}_a \sim t$  curve close to the melting point. It should be noted that this assumption does not introduce a serious error for

the following discussions, because  $\bar{V}_a$  thus calculated for any of the samples from (3) does not deviate more than 0.01ml/g for generally accepted  $\bar{V}_a$  at about 140°C.

#### E. X-ray Diffraction (Wide Angle)

A General Electric XRD-5 diffractometer with a copper target tube was used throughout the experiment. For the determination of (110) and (200) spacings, 0.4° beam slit and 0.05° detector slit were chosen, along with a slow scanning speed (0.2°/min). Peak angles were calibrated with NaCl powder as reference. The conditions employed for the crystallinity determination are: 0.4° beam slit, 0.1° detector slit and scanning speed 2°/min. The method described by Hindus and Schnell<sup>34</sup> was followed to calculate crystallinity from the x-ray diffraction intensity. In either case a flat surface was carefully cut out of the sample to assure satisfactory diffraction trace.

XRD powder camera with effective film diameter 14.32cm was used in some cases to check changes in crystal structure of the samples by pressure. A thin rod (diameter less than 1/2mm) was cut from the sample and mounted in the camera with clay. The sample was rotated slowly at the center of the camera.

F. Small Angle X-ray Scattering and Electron Microscopy

Measurement of long periods in the samples and electron microscopy on fracture surfaces were carried out by P. H. Geil at the Camille Dreyfus Laboratory and F. R. Anderson at the Chemstrand Research Center in Durham, North Carolina.

A Jarrell-Ash-Frank Optically Focussing Small Angle X-ray Camera with a resolution of about 500A was used to get small angle patterns.

Electron microscopy observation was done on thin replicas of the fracture surfaces. The samples were fractured at liquid nitrogen temperature. Samples 14 and 15, which are highly crystalline and brittle, were easily fractured at room temperature. Following the fracture, the surfaces were shadowed with platinum under vacuum. The replicas were then removed from the samples using polyacrylic acid, backed with carbon and used for the observation. The details of these techniques are described elsewhere.<sup>8</sup>

G. Calorimetry

Calorimetric measurement of sample 31-39 was carried out at Rensselaer Polytechnic Institute, Troy, New York. A Perkin-Elmer Differential Scanning Calorimeter was used. 5 to 10mg of samples which were weighed to  $\pm 10$  microgram was placed in an aluminum pan, encapsulated by sealing the pan with an aluminum cover, and transferred to the sample holder.

An empty pan was placed on the reference holder. A programmer controlled the heating in such a manner that the average temperature of the sample and the reference were raised at the rate of 2.5°C/min. The differential temperature controller responded to the temperature difference between the sample and the reference, nullifying it by adjusting the differential power increment fed to the reference and sample heaters. A signal proportional to the differential power was recorded on the chart against the average temperature. The temperature of the sample was calibrated against the melting points of indium and triphenylmethane. The area under a peak in the chart is proportional to the heat added during the melting process of the sample. Sample 33, with density crystallinity 99%, was used as the standard sample to obtain the heat of fusion.  $\Delta H$  was assumed to be 66cal/g for this standard sample.

#### H. Materials

The polymers used in the experiment are described below. All polymers are crystallized without further fractionation.

##### Polymethylene

A commercially available polymethylene was used. The polymer was obtained from diazomethane without a prohibitor. The molecular weight of the polymer is very high. (The supplier, Microtek Company, Baton Rouge, Louisiana, estimated

it at about 14 million.) Sample 31 corresponds to this polymer.

### Polyethylenes

Polymers A and B belong to different lots of linear polyethylene (Marlex 50) which was polymerized with calcinated chromium oxide catalyst. The samples were generously provided by the Phillips Petroleum Company. P<sub>1</sub> is another linear low-pressure polyethylene, supplied by the Research Department of the Hercules Powder Company.

The characterizations of these three polyethylenes as well as ethylene-butene copolymers was carried out by the use of Gel Permeation Chromatography.<sup>36</sup> Full credit for the characterization goes to Dr. B. A. Denenberg of Waters Associations, Inc.

The results are shown in Table II and Fig. 4. The last column of the table shows the numbers of the samples corresponding to each polymer.

In Gel Permeation Chromatography, the separation of molecules is primarily done with respect to molecular size, and therefore molecular weight distribution is given as weight fraction vs molecular length. The data in Table II were calculated assuming a weight of 11.20g/A mole for polyethylene.

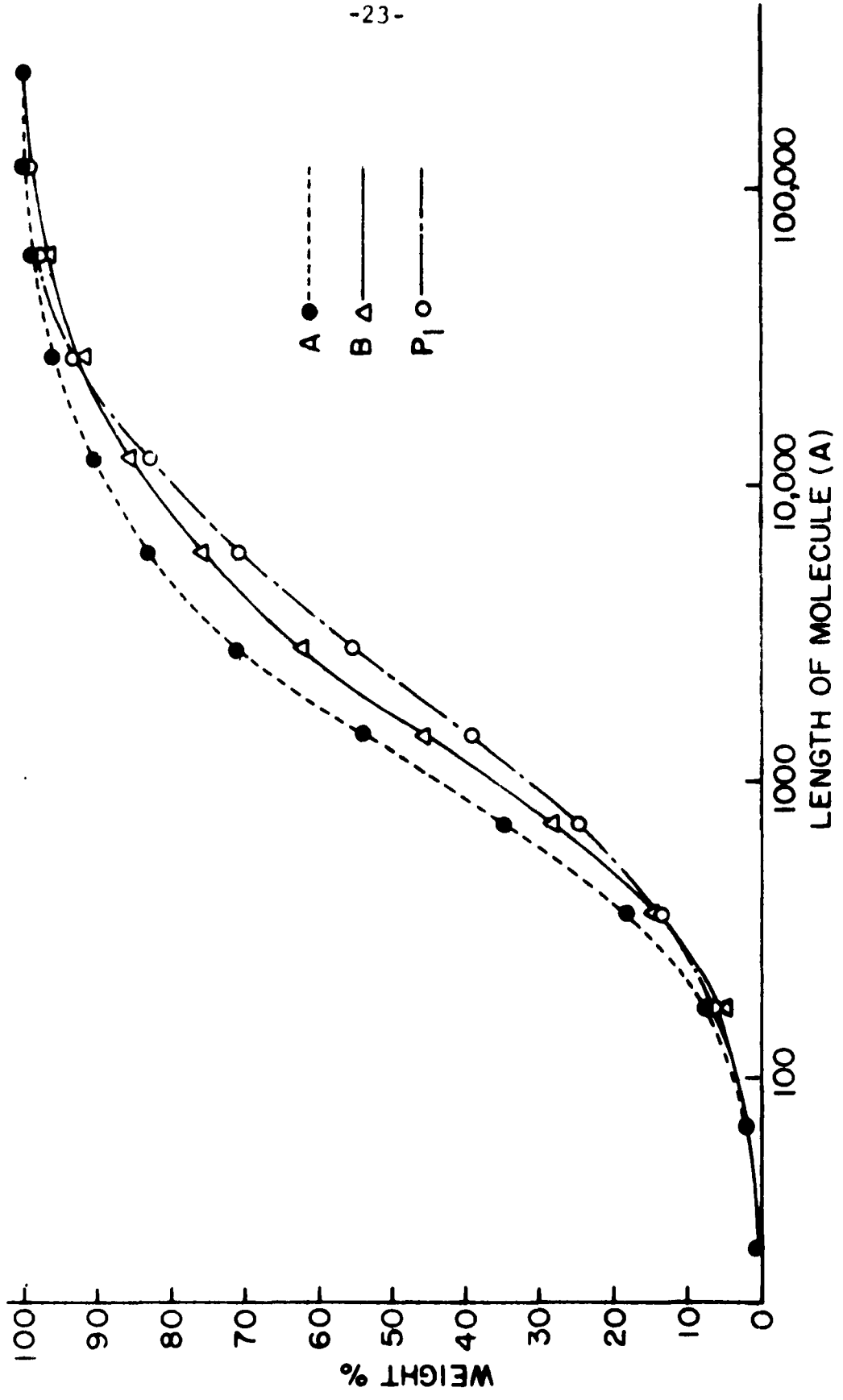


Figure 4. Cumulative molecular length distribution of polyethylenes.

TABLE II. MOLECULAR WEIGHT OF POLYETHYLENES

Polymer	$\bar{M}_n$	$\bar{M}_w$	$\bar{M}_w/\bar{M}_n$	Corresponding sample numbers
A	8,200	80,000	10	27-30, 32
B	8,900	140,000	16	1-26
P <sub>1</sub>	9,800	130,000	13	33

#### Ethylene-Butene-1 Copolymers

Four copolymers of ethylene and butene-1, which are labelled B-1 to B-4, were kindly supplied by the Research Department of the Hercules Powder Company. They were polymerized by a low pressure process and are linear polymers with ethyl group branches only. The polymer compositions as determined by the supplier are given in Table III, along with the molecular weight information and the corresponding sample numbers. The molecular length distributions of the polymers are shown in Fig. 5.

To calculate molecular weight from molecular length, 11.27, 11.40, 11.42 and 11.58g were assigned to 1A mole of B-1, B-2, B-3 and B-4 polymer chains, respectively, based on the assumption that branches are randomly distributed and do not contribute to the chain length.

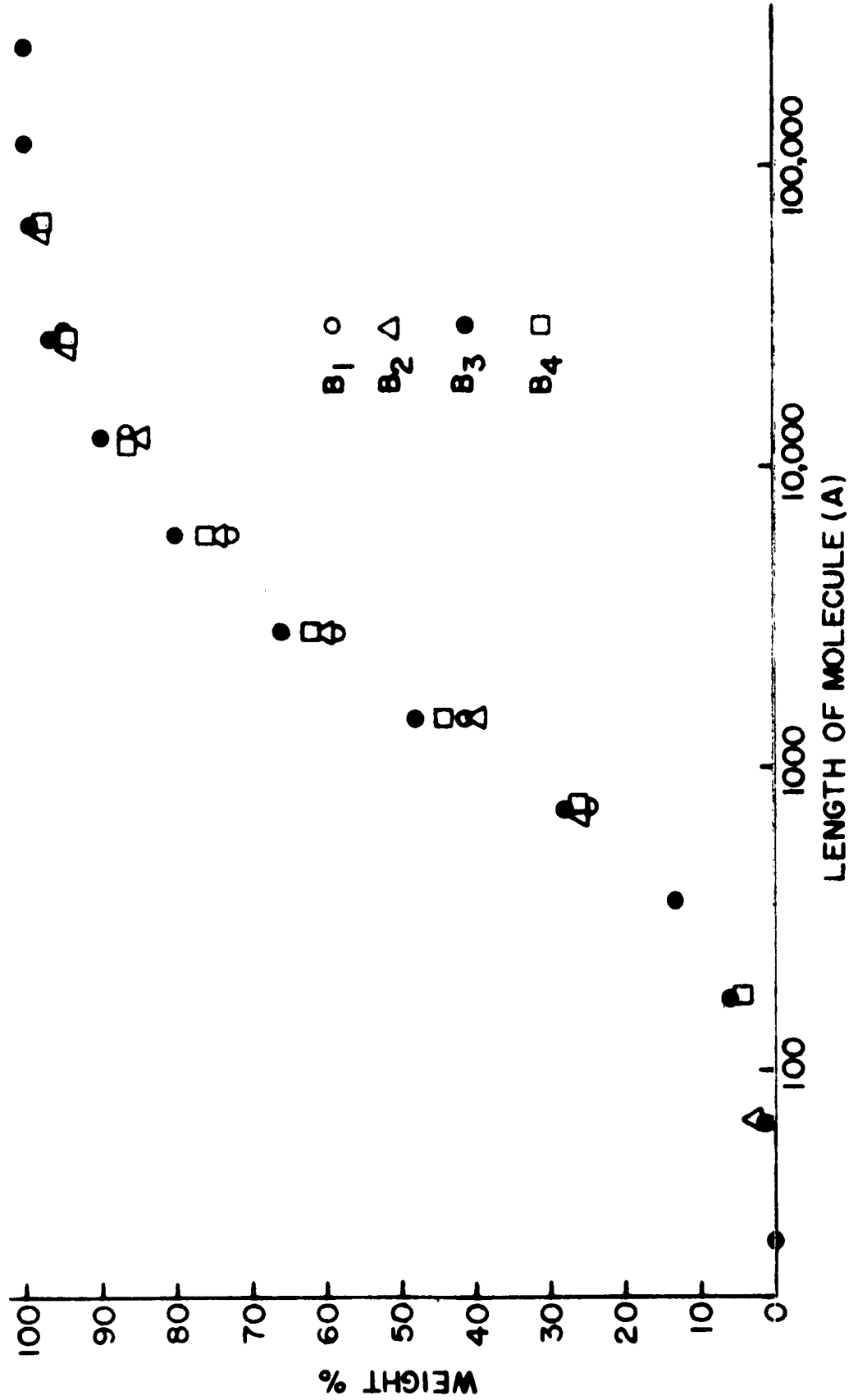


Figure 5. Cumulative molecular length distribution of ethylene-butene-1 copolymers.

TABLE III. PROPERTIES OF ETHYLENE-BUTENE-1 COPOLYMERS

Polymer	C <sub>2</sub> Branches per 100C	$\bar{M}_n$	$\bar{M}_w$	$\frac{\bar{M}_w}{\bar{M}_n}$	Corresponding sample numbers
B-1	0.3	11,000	110,000	9.7	34
B-2	0.9	9,100	120,000	13.0	35
B-3	1.0	10,000	88,000	8.6	36
B-4	1.7	10,000	120,000	12.0	37

Ethylene-Propylene Copolymers

Two ethylene-propylene copolymers, P<sub>2</sub> and P<sub>3</sub>, were also supplied by the Research Department of the Hercules Powder Company. They were polymerized with a low pressure catalyst. Their properties as determined by the supplier are shown in Table IV along with the corresponding sample numbers.

TABLE IV. DESCRIPTION OF ETHYLENE-PROPYLENE COPOLYMERS

Polymer	Ch <sub>3</sub> /100C	Viscosity number	Corresponding sample numbers
P <sub>2</sub>	0.2	3.3	38
P <sub>3</sub>	0.7	3.0	39

### III. RESULTS

#### A. Linear Polyethylene

##### a) DTA, Density and Wide Angle X-ray Diffraction

Table V shows the results of density, x-ray and DTA measurements done on linear polyethylene samples which had been crystallized under the indicated conditions. Polyethylene B was used for all these experiments (See II-H for the sample description).  $\Delta T$  in the table was calculated by the use of the equation

$$\Delta T = t_m^{\circ} + 0.02p_c - t_c \quad (4)$$

where  $t_m^{\circ}$  is the equilibrium melting point of linear polyethylene at atmospheric pressure and was assumed to be  $142^{\circ}\text{C}$ . Then  $t_m^{\circ} + 0.02p_c$  is the approximate melting point at  $p_c$  (atm).  $\Delta T$  represents the degree of supercooling of the sample, assuming that they consist of infinitely long, unbranched polyethylene molecules. The first group of 15 samples was crystallized at a constant degree of supercooling ( $12^{\circ}\text{C}$ ), while the samples in the second group were crystallized at a constant temperature under various pressures, and accordingly at different degrees of supercooling. Negative  $\Delta T$  indicates that no crystallization should occur during the initial pressurization, while large positive  $\Delta T$  indicates quick quenching on application of pressure. All samples were

TABLE V.

## DATA OF POLYETHYLENE CRYSTALLIZED UNDER DIFFERENT PRESSURES

Sample	Cryst. Conditions				Density	
	Temp. $t_c$ (°C)	Press. $p_c$ (atm)	Time hours	$\Delta T$ °C	$d(25)$ g/ml	Cryst. %
1	130	1	8	12.0	0.980	89
2	130	1	8	12.0	0.979	88
3	140	480	9	11.6	0.979	88
4	150	985	8	11.7	0.980	89
5	160	1530	18	12.6	0.981	89
6	170	2000	8.5	12.0	0.983	90
7	176	2300	8	12.0	0.980	89
8	181	2580	8	12.6	0.979	88
9	186	2760	8	11.0	0.986	92
10	186	2860	8	13.2	0.980	89
11	191	3060	8	12.2	0.984	91
12	201	2540	8	11.8	0.991	95
13	206	3810	8	12.2	0.991	96
14	226	4800	8	12.0	0.994	97
15	236	5300	49	12.0	0.992	96
16	170	1	0	-28.0	0.977	87
17	170	740	0	-13.3	0.980	88
18	170	1290	0	-02.2	0.981	89
19	170	1290	0	-02.2	0.982	90
20	170	1940	0	+10.8	0.980	88
21	170	2580	0	23.6	0.976	86
22	170	2580	0	23.6	0.973	85
23	170	3880	0	49.6	0.983	91
24	170	3880	0	49.6	0.985	92
25	170	5170	0	75.4	0.983	90
26	170	5170	0	75.4	0.983	90

TABLE V (cont.)

Sample	X-ray Measurement			DTA			
	(110) Spacing	(200) Spacing	Cryst.	Begin- ning of Melting	Low Temp. Peak	High Temp. Peak	Extrap. max. mp
	A	A		°C	°C	°C	°C
1	4.12	3.72	89	---	---	---	---
2	--	--	--	117.3	133.7	---	134.8
3	4.12	3.72	86	119.4	134.1	---	135.7
4	4.12	3.72	90	118.7	135.0	---	136.1
5	4.12	3.72	90	119.9	133.9	---	135.6
6	4.13	3.72	91	118.6	135.2	---	136.6
7	--	--	--	126.1	133.4	---	134.8
8	--	--	88	124.6	133.2	---	134.5
9	--	--	91	124.5	133.2	138.5	---
10	4.13	3.72	88	124.9	133.6	138.1	139.0
11	--	--	91	120.7	132.5	137.4	138.5
12	--	--	95	122.6	130.5	137.6	139.6
13	4.12	3.72	95	113.4	130.5	137.6	139.6
14	4.12	3.72	97	114.7	*	138.8	140.1
15	--	--	96	121.1	*	138.8	139.9
16	--	--	--	---	---	---	---
17	--	--	--	120.0	134.6	---	135.9
18	4.12	3.71	--	119.0	134.6	---	135.7
19	--	--	--	117.4	134.8	---	135.7
20	4.11	3.71	--	---	135.5	---	136.4
21	4.12	3.72	--	121.8	133.6	---	135.2
22	--	--	--	115.0	134.4	---	137.4
23	4.12	3.72	--	111.2	129.3	137.9	139.4
24	--	--	--	115.7	129.4	136.6	138.5
25	4.13	3.72	--	115.1	---	135.7	137.2
26	--	--	--	118.3	*	138.5	140.5

cooled after the number of hours shown in column 4 at a rate of 4°C/hr. Any material which did not crystallize at the initial  $t_c$  and  $p_c$  has crystallized at a lower temperature, but at initial  $p_c$ . Asterisks in the low temperature peak column for some of the samples mean that those samples show several small peaks instead of one low temperature peak.

Figure 6 shows five representative DTA traces illustrating the changes occurring in going from the low pressure crystallization to the high pressure crystallization. Increasing pressure produces increasing amounts of high temperature-melting crystals, which finally dominate the whole sample. It will be shown later that this high pressure-crystallized polymer is of extended chain morphology, contrary to the atmospheric pressure-crystallized polyethylene, which is always of folded chain morphology. In all the DTA traces,  $\Delta T$  is shown in arbitrary units. A larger  $\Delta T$  means a higher temperature of the reference with respect to the sample.

In Fig. 7 three DTA curves are compared to show the dependence of the crystallite size distribution on the degree of supercooling. Increasing sample number indicates a higher degree of supercooling (see Table V).

Figure 8 shows a "step-wise" DTA measurement on sample 15 to investigate the nature of its three low temperature peaks found in normal DTA measurement (curve A). In this experiment

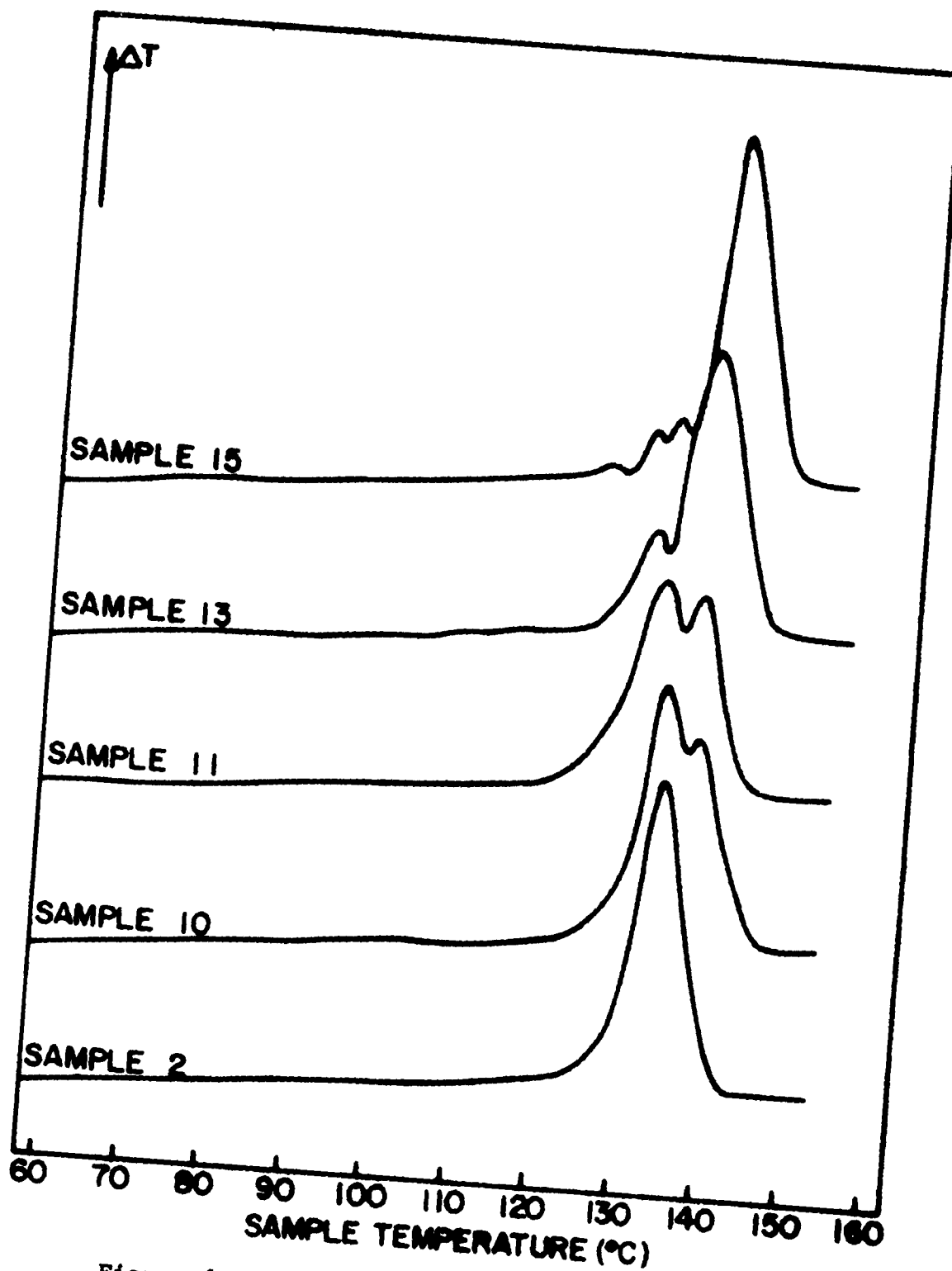


Figure 6. DTA traces of polyethylene samples crystallized under elevated pressure.

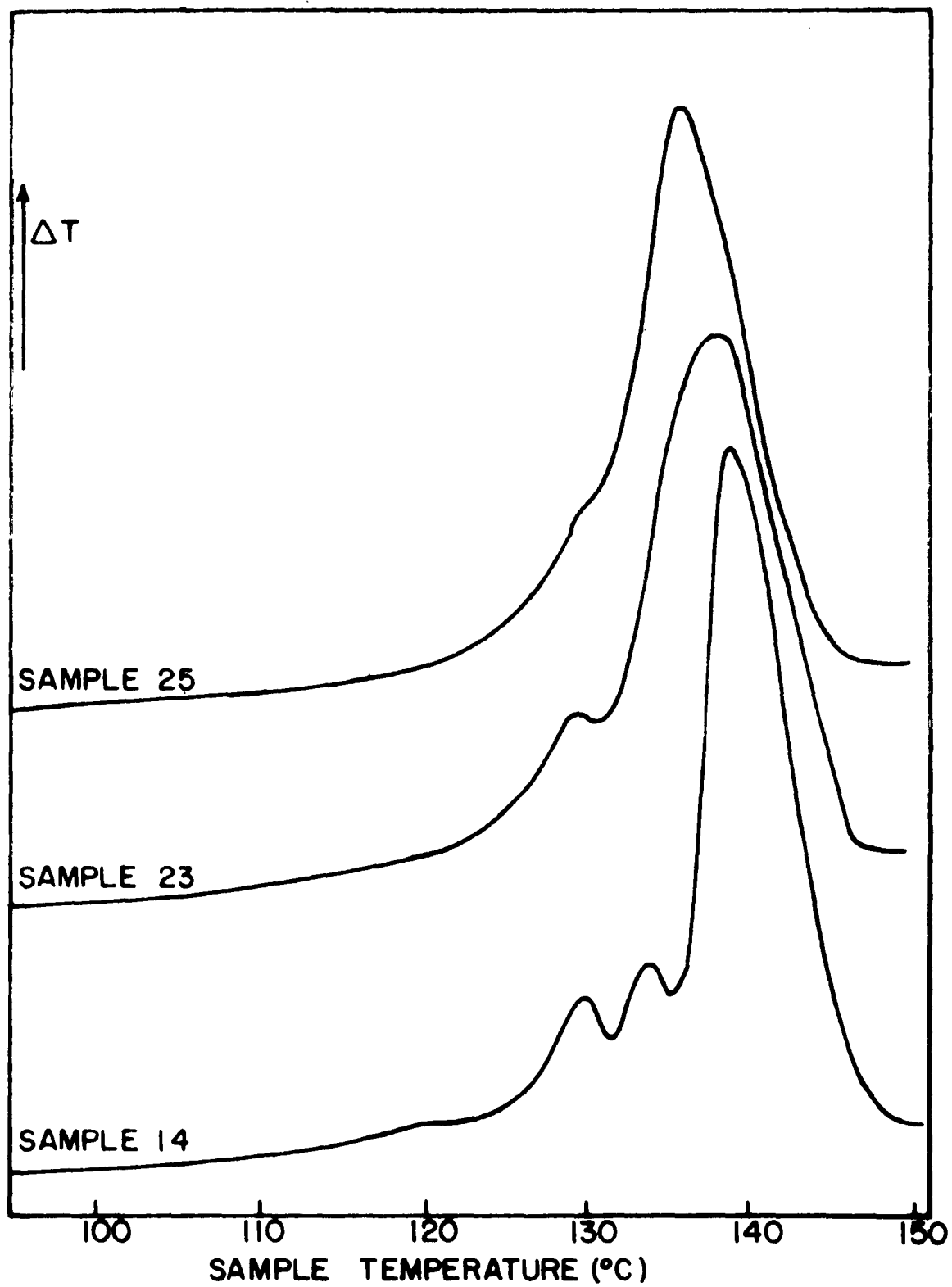


Figure 7. DTA traces of polyethylene crystallized at high pressure.

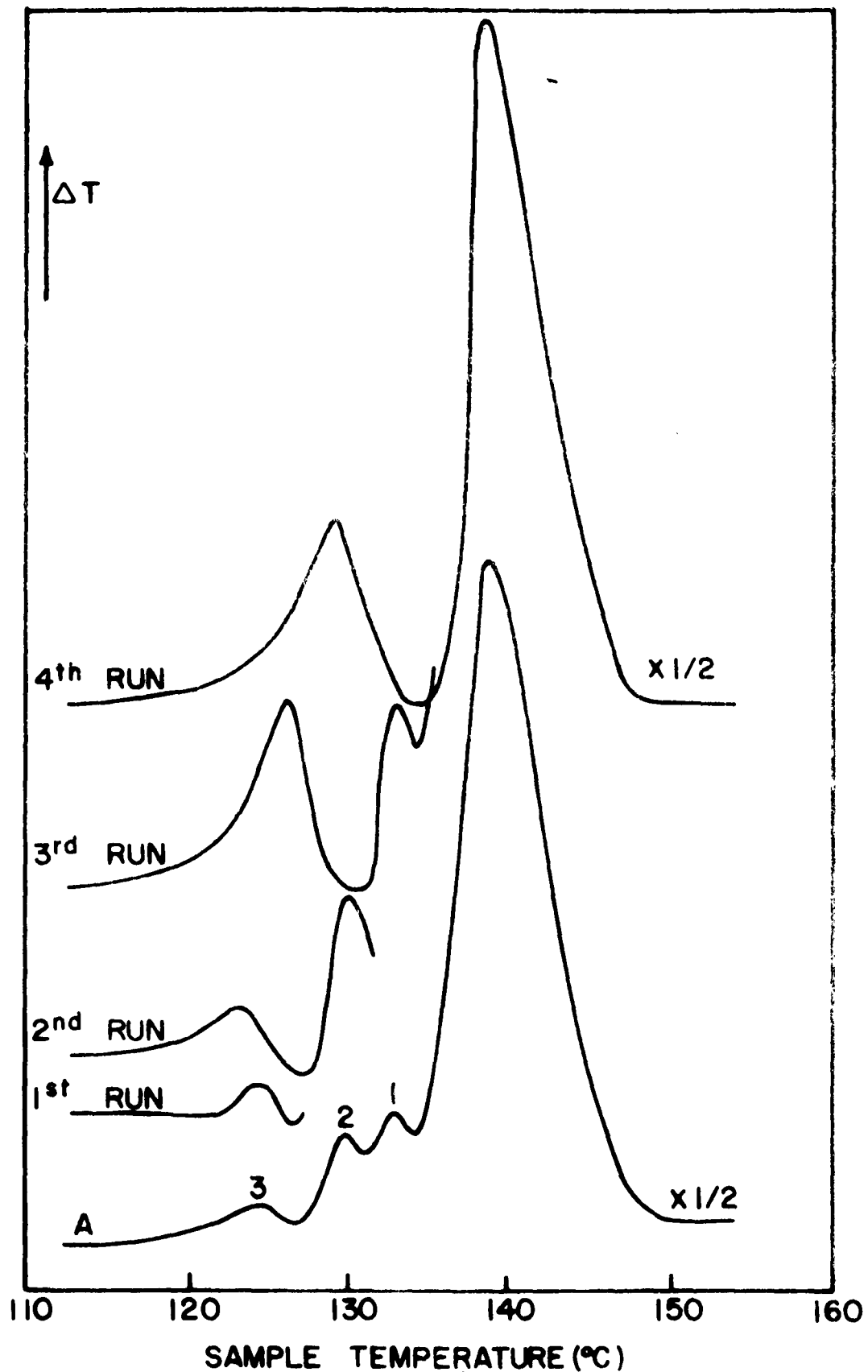


Figure 8. Step-wise DTA of sample 15.

the first run of DTA was stopped when the first low temperature peak was reached. The sample holder was then cooled to room temperature in air. In the second run heating was continued until the second low temperature peak was completely recorded. This procedure was repeated for all four peaks including the high temperature peak. The normal and final DTA traces are shown at 1/2 the  $\Delta T$  scale for runs 1, 2, and 3.

In Fig. 9 extrapolated melting temperatures are plotted from the DTA of all the samples. Analyses of melting peaks lower than 125°C are omitted. Circles correspond to samples 1-15, while the squares are used for samples 16-26. Smaller circles and squares show the analysis of minor peaks and shoulders. When the extrapolation procedure for the melting point is not possible, peak temperatures are used instead for the secondary peaks. They are designated by filled circles and squares.

Figure 10 shows the relation between density and crystallization pressure for both groups of the samples.

The crystallinity obtained by means of x-ray diffraction is plotted against the crystallinity by density in Fig. 11. The drawn-in line represents one to one correspondence.

#### b) Electron Microscopy and Low Angle X-ray Diffraction

Electron microscopy observation, electron diffraction observation and small angle x-ray diffraction were carried

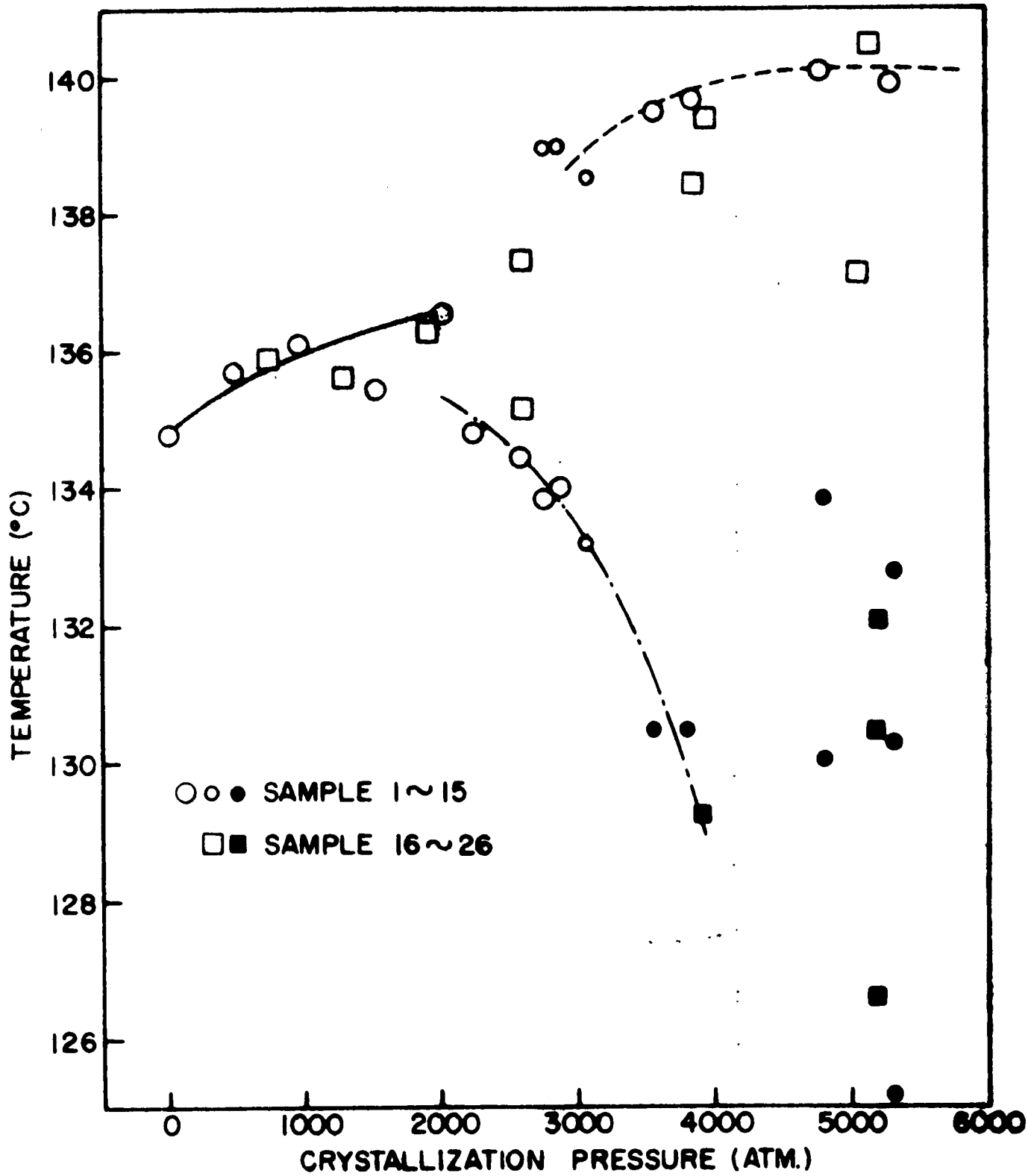


Figure 9. Experimental maximum melting points of pressure-crystallized polyethylene.

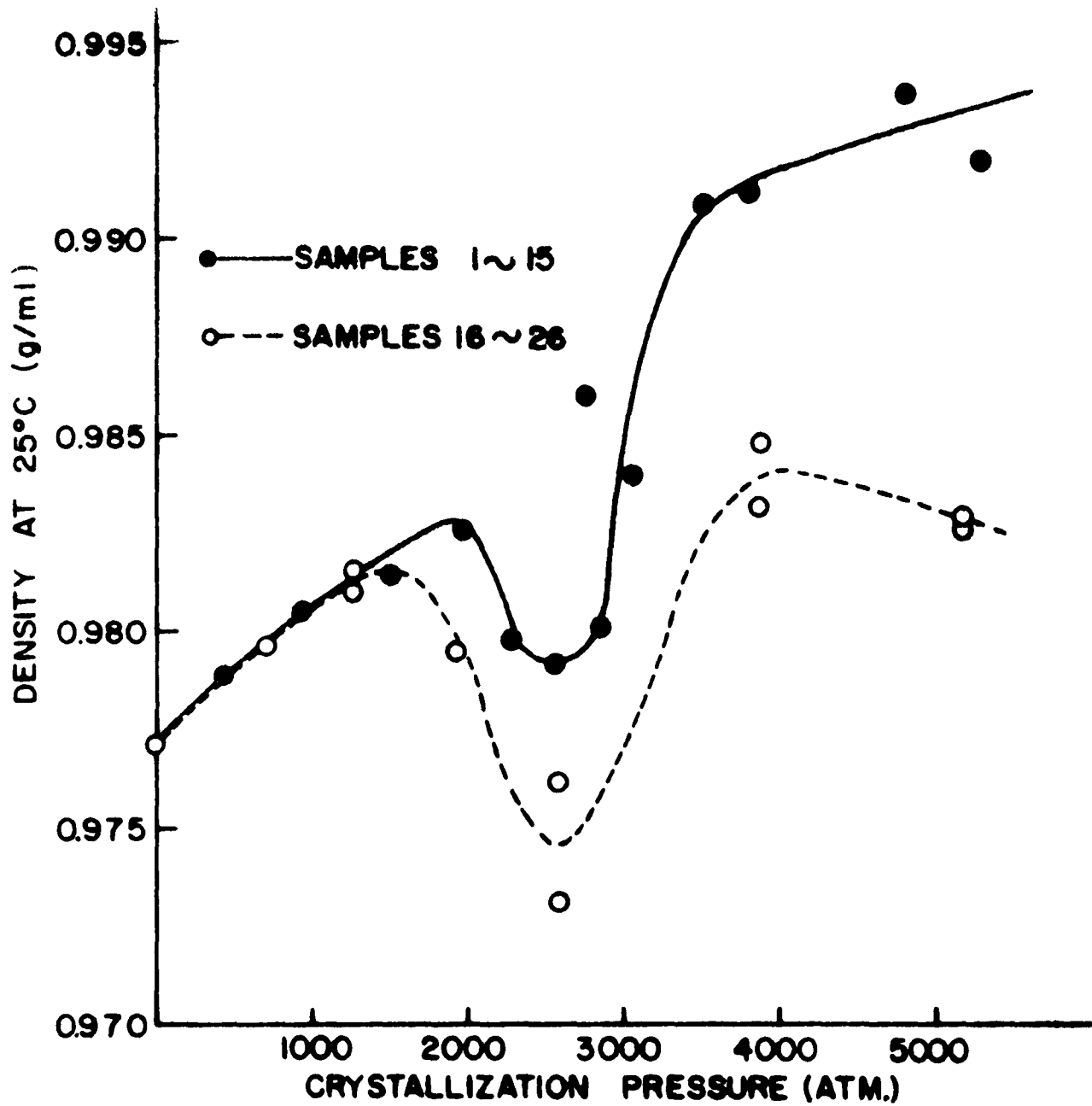


Figure 10. Density of polyethylene crystallized under elevated pressure.

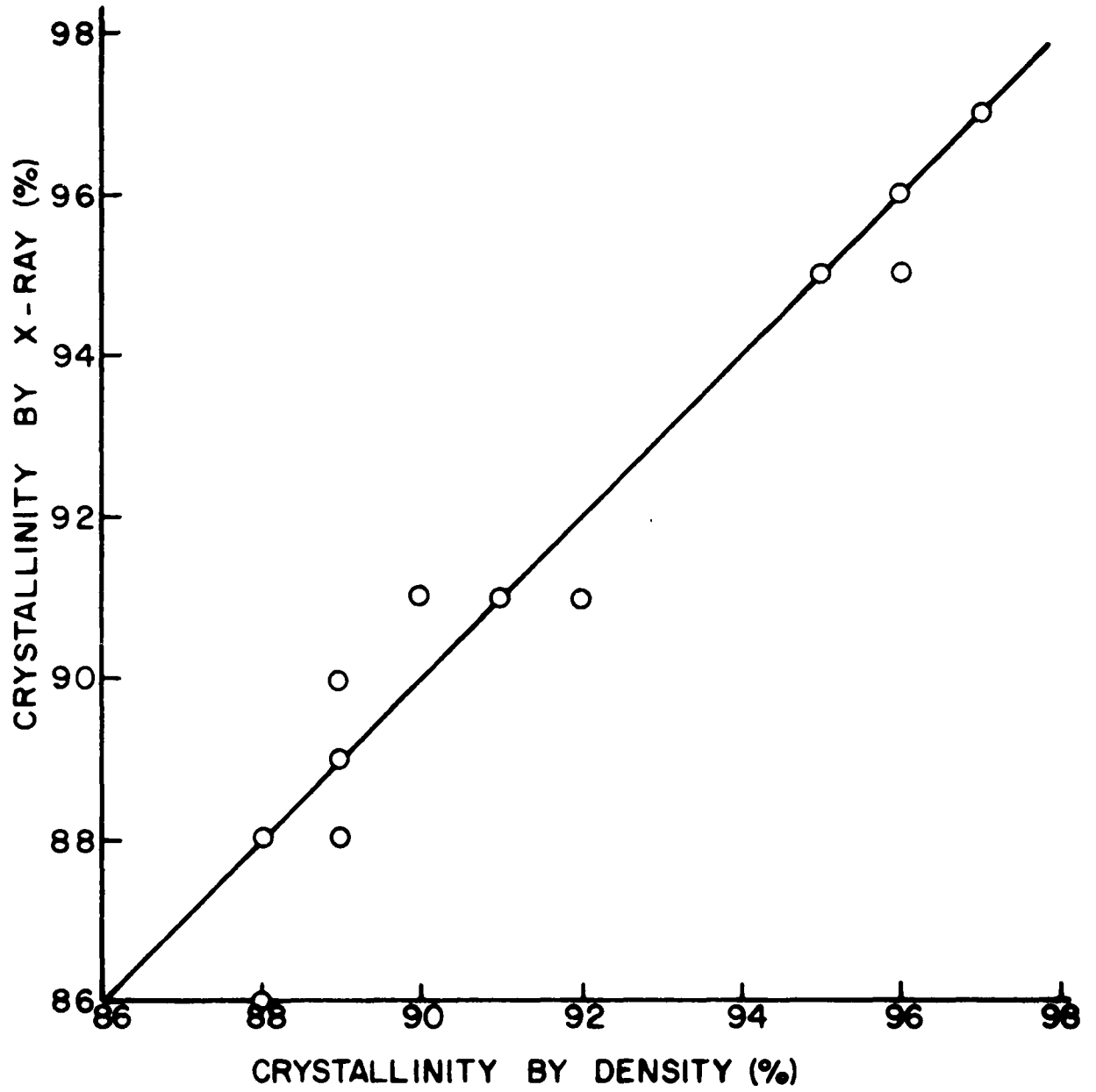


Figure 11. Relation between x-ray crystallinity and density crystallinity.

out on samples 1, 6, 9, 14, and 15 by Anderson and Geil<sup>39</sup> in the laboratories of the Chemstrand Corporation and the Research Triangle Institute, Durham, North Carolina.

The results of small angle diffraction are shown in Table VI.

TABLE VI. SMALL ANGLE DIFFRACTION

<u>Sample</u>	<u>Long Period</u>	<u>Cryst. Pressure</u>
1	400A	1 atm
6	600A	2000 atm
9	400A	2760 atm
14	} No discrete or diffuse scattering }	4800 atm
15		5300 atm

Figure 12 shows electron micrographs of replicas of fracture surfaces of samples 6, 14 and 15, and an electron diffraction pattern of a portion of a lamella adhering to the replica of sample 14. The diffraction pattern corresponds to the black outlined area in the (unfortunately) somewhat poorly focussed electron micrograph.

The fracture surfaces of sample 1 are similar to those found previously. Irregular, fibrillar structure covers much of the surface, indicating the presence of type I or folded chain lamellae.\* In a few regions, areas on the order

---

\* For the description of type I, II, III lamellae, see Chapter IV.

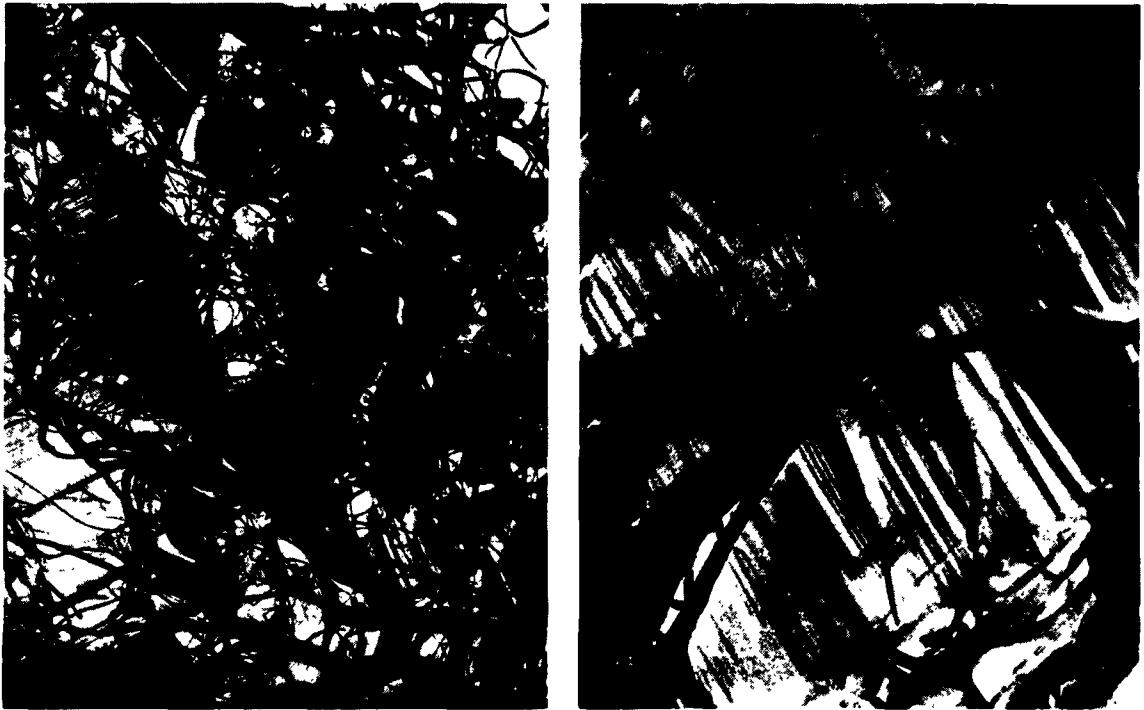


Figure 12. Electron micrographs and selected area diffraction pattern of pressure-crystallized polyethylene.

of  $100\mu$  were observed. In that area type III lamellae which had a thickness of between 300A and 600A, averaging 380A, were present.

Considerably larger portions of samples 6 and 9 were found to consist of type III lamellae. Folded chain lamellae were also observed in both cases. Type III lamellae in sample 6 (see Fig. 12A) vary in thickness between 200A and 1,000A, averaging 480A. Sample 9 has a similar appearance. In this sample, however, the thickness of type III lamellae ranges from 300A to 3,000A, with an average of 800A. The thicker lamellae in sample 9 resemble the bands observed in highly crystalline polytetrafluoroethylene,<sup>37</sup> while the thinner ones are similar in appearance to the structure observed in moderately crystalline polytetrafluoroethylene.<sup>38</sup> It was observed that striations in sample 6 often made an angle other than  $90^\circ$  with the lamellae; they also appeared more closely spaced than those in sample 9.

In both sample 14 (Fig. 12C) and sample 15 (Fig. 12B), the entire fracture surface is occupied by type III lamellae of various thicknesses. In both samples optical microscope observation indicates that the lamellae are organized in incipient spherulites or in sheaf-like clusters. This can also be seen in the low magnification electron micrograph (Fig. 12B). Lamellae with thicknesses up to  $3\mu$  have been observed in samples 14 and 15. The average thickness of the

lamellae is about 2,500Å. The striations in these samples are continuous across an entire lamella. In some cases, the fracture surface changes levels, and it appears that the striations correspond to the fracture edges of the sheet-like structures which were suggested by Speerschneider and Li.<sup>38</sup> In Fig. 12C both "fiber" structures and kinks can be observed. Fibers seem to have been detached from the sheets. Most of them are several hundred angstroms in diameter and their length is equal to the corresponding lamellar thickness. Kinks seem to be peculiar to the thicker type III lamellae, and they often accompany related changes in the fracture plane.

#### B. Polymethylene and Polyethylene Copolymers

##### a) DTA, Density, Dilatometry, and Calorimetry

Crystallization at high pressure was also carried out with some other polymers.

The results of density, DTA, dilatometry and calorimetry measurements on these samples are summarized in Table VII. (For identification of the samples, see II-H.) The samples were kept at the temperatures and pressures described in the table for 20 hours and then cooled to room temperature at the rate of 1.6°C/hr. The crystallization conditions were such that all the crystallizations, except those of the

TABLE VII  
 DATA OF POLYMETHYLENE, POLYETHYLENES, AND POLYETHYLENE COPOLYMERS  
 CRYSTALLIZED AT HIGH PRESSURE

Sample	Cryst. Conditions		Density $d^{25}$ (g/ml)	Cryst. %	Begin- ning of melting °C	DTA				
	Temp. °C	Pressure atm				Side peaks			Main peak	
						Peak Temp. °C	Peak Temp. °C	Peak Temp. °C	Peak Temp. °C	Extrap. Temp. °C
31	227	4760	0.995	97	---	---	---	---	---	---
32	227	4800	0.995	97	120.4	---	131.1	133.8	139.8	141.1
33	227	4350	0.997	99	124.7	---	130.5	134.3	139.8	140.9
34	227	4350	0.989	94	121.2	---	128.3	134.2	139.3	140.3
35	227	4760	0.960	76	98.9	---	121.9	131.0	138.7	139.8
36	227	4900	0.949	69	71.7	---	121.6	130.0	137.8	139.1
37	227	4300	0.938	62	68.7	107.8	122.8	133.5	140.3	141.1
38	227	4350	0.988	93	---	---	---	132.7	138.7	140.0
39	227	4100	0.968	81	---	---	---	---	---	---

TABLE VII (cont.)

Sample	Melting Point by Dilatometry (°C)	First Perceptible Deviation (°C)	Side Peaks (°C)	Calorimetry			
				Peak Temp. (°C)	Main Peak Return to equil. (°C)	ΔH (Cal/g)	Cryst. %
31	141.4	139.5	none	150.2	152.5	59.0	89
32	138.7	121.5	132.2	142.7	144.1	59.7	90
33	138.7	124.5	132.7	144.7	146.5	66.0	99
34	138.4	119.0	130.7	144.2	145.5	56.8	85
35	138.2	108.5	123.2	140.0	140.5	40.6	61
36	137.2	106.5	125.2	141.4	143.3	38.3	57
37	138.6	94.5	125.2	143.2	144.5	32.9	49
38	137.5	121.5	127.2	141.4	143.5	57.3	86
39	137.5	107.5	122.2	140.6	141.5	43.4	65

polyethylenes, took place during the process of cooling, thus allowing all copolymers to crystallize under similar conditions.

The same crystallization procedure was employed for the crystallization of Marlex 50 and the results indicate that the initial temperature of crystallization does not affect the property of the sample seriously, so long as the initial degree of supercooling is not very high and the pressure is maintained higher than 4,000atm (see Table VIII).

TABLE VIII. DEPENDENCE OF THE DENSITY OF MARLEX 50 ON CRYSTALLIZATION TEMPERATURE AT A CONSTANT CRYSTALLIZATION PRESSURE OF 4,300ATM.

<u>Sample</u>	<u>Temp. (°C)</u>	<u>ΔT(°C)</u>	<u>d(g/ml, 25°C)</u>
27	187	41	0.991
28	207	21	0.993
29	217	11	0.993
30	227	1	0.993

Figure 13 shows DTA traces of polyethylene and ethylene-butene copolymers. A smaller amount of sample was used for sample 33 to avoid scaling out, and therefore its peak would be sharper if the same amount of sample as the others had been used.

As is clearly shown in Table VII, there is a discrepancy between the melting points found by dilatometry and those by

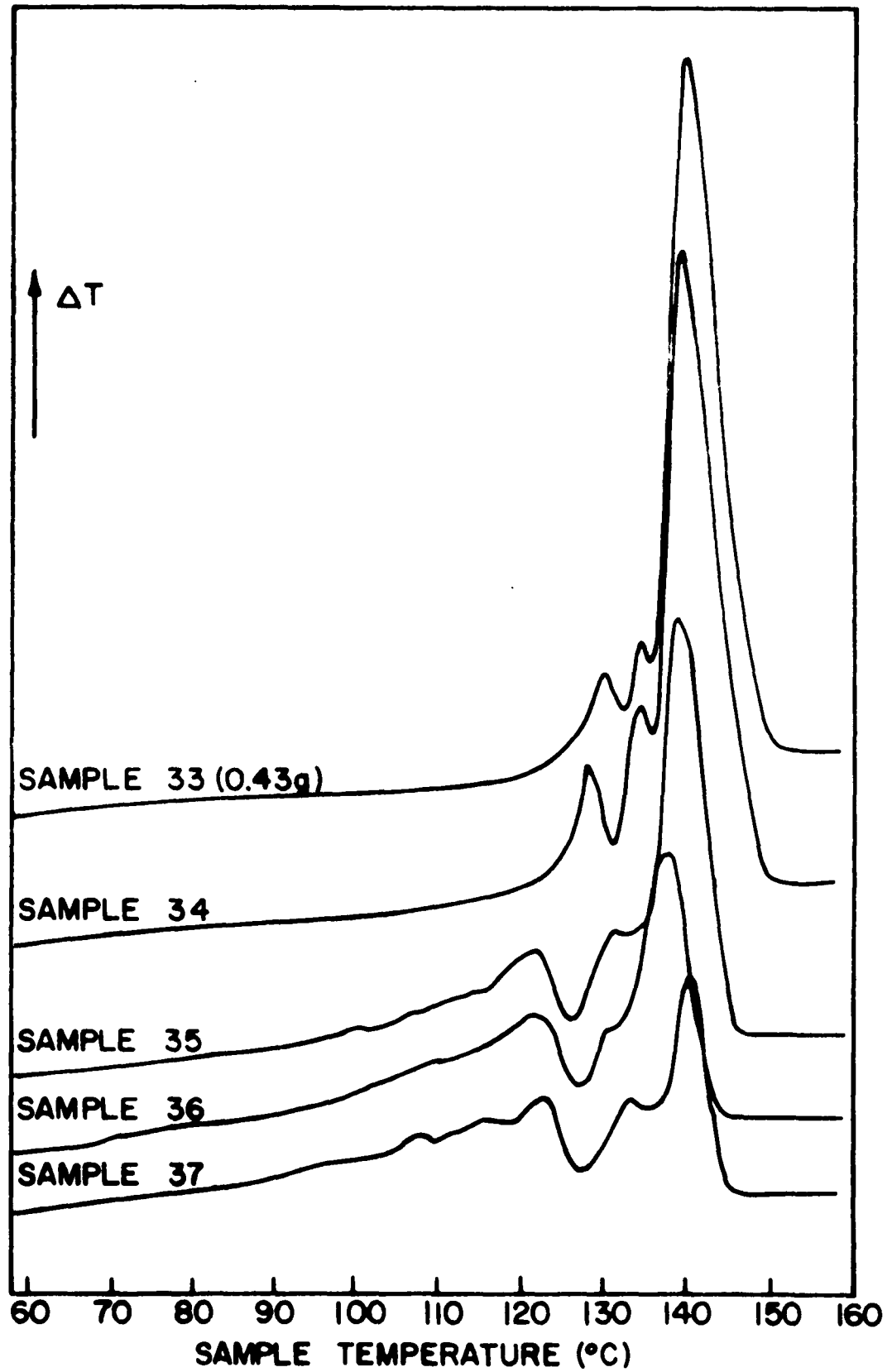


Figure 13. DTA traces of polyethylene copolymers crystallized at high pressure.

DTA. In order to elucidate this phenomenon, the dependence of DTA peak temperatures on the rate of heating was studied with samples 31, 32 and 37. The results appear in Fig. 14. The curve gives evidence of superheating of these samples.

The results of dilatometry of samples 31-39 are summarized in Tables IX to XVII. Common  $\bar{V}$ -T relations are illustrated for all these samples in Figs. 15 to 17. The melting points are shown by arrows in the figures, and they are also listed in Table VII.

#### b) Electron Microscopy

Figure 18 shows two electron micrographs of the fracture surfaces of sample 31 (polymethylene). Generally, the fracture surfaces of this sample resemble those observed for polyethylenes with extended chain structure, except that lamellas in sample 31 are thicker (large ones reach  $6\mu$ ) and that the very thin lamellae which are abundant in the polyethylenes are seldom observed.

As Fig. 13 shows, the surfaces of these samples are much more fibrous than those of polyethylenes (samples 14 and 15), and the fibers are generally far longer than the thicknesses of the lamellae from which they have been pulled out. More disordered regions can be observed between the thick lamellae.

TABLE IX

DILATOMETRY OF SAMPLE 31

<u>Temp.</u> <u>(°C)</u>	<u><math>\bar{V}</math></u> <u>(ml/g)</u>	<u><math>W_c</math></u> <u>—</u>
25.0	1.0052	0.973
40.5	1.0087	0.980
51.4	1.0121	0.980
65.0	1.0173	0.975
85.0	1.0250	0.967
97.0	1.0297	0.964
111.8	1.0364	0.953
119.4	1.0376	0.959
124.3	1.0421	0.946
128.5	1.0436	0.945
130.3	1.0445	0.944
132.2	1.0468	0.936
134.3	1.0488	0.930
135.3	1.0497	0.928
136.4	1.0512	0.922
137.5	1.0537	0.913
138.7	1.0614	0.880
139.8	1.0827	0.787
140.9	1.2133	0.207
141.9	1.2606	0.000
142.7	1.2618	
144.0	1.2633	
151.1	1.2700	
152.9	1.2717	

TABLE X  
DILATOMETRY OF SAMPLE 32

<u>Temp.</u> <u>(°C)</u>	<u><math>\bar{V}</math></u> <u>(ml/g)</u>	<u><math>W_c</math></u> <u>—</u>
25.0	1.0055	0.970
40.5	1.0096	0.975
51.4	1.0130	0.978
65.0	1.0175	0.974
85.0	1.0252	0.979
97.0	1.0314	0.957
111.8	1.0405	0.936
119.4	1.0476	0.916
124.3	1.0529	0.900
128.5	1.0603	0.874
130.3	1.0676	0.845
132.2	1.0754	0.815
134.3	1.0876	0.766
135.3	1.0914	0.751
136.4	1.1036	0.701
137.5	1.1528	0.492
138.7	1.2683	0.002
139.8	1.2695	0.000
140.9	1.2705	
141.9	1.2714	
142.7	1.2721	
144.0	1.2733	
151.1	1.2798	
152.9	1.2816	

TABLE XI

DILATOMETRY OF SAMPLE 33

<u>Temp.</u> <u>(°C)</u>	<u><math>\bar{V}</math></u> <u>(ml/g)</u>	<u><math>W_c</math></u> <u>—</u>
25.0	1.0027	0.987
40.5	1.0070	0.989
51.4	1.0100	0.991
65.0	1.0141	0.992
85.0	1.0217	0.984
97.0	1.0276	0.975
111.8	1.0348	0.961
119.4	1.0390	0.953
124.3	1.0422	0.945
128.5	1.0488	0.922
130.3	1.0556	0.893
132.2	1.0655	0.852
134.3	1.0763	0.807
135.3	1.0841	0.773
136.4	1.0982	0.712
137.5	1.1359	0.546
138.7	1.2581	0.004
139.8	1.2598	0.000
140.9	1.2610	
141.9	1.2620	
142.7	1.2627	
144.0	1.2636	
151.1	1.2700	
152.9	1.2720	

TABLE XII  
DILATOMETRY OF SAMPLE 34

<u>Temp .</u> <u>(°C)</u>	<u><math>\bar{V}</math></u> <u>(ml/g)</u>	<u><math>W_c</math></u> <u>—</u>
25.0	1.0113	0.937
40.4	1.0162	0.938
50.0	1.0197	0.936
60.1	1.0255	0.923
70.1	1.0277	0.929
79.6	1.0322	0.923
90.1	1.0385	0.909
99.7	1.0448	0.894
105.6	1.0491	0.884
110.1	1.0521	0.877
114.0	1.0562	0.865
116.0	1.0584	0.858
120.0	1.0635	0.841
123.3	1.0682	0.825
125.9	1.0745	0.801
127.6	1.0815	0.772
129.4	1.0893	0.740
130.2	1.0911	0.734
131.2	1.0932	0.726
132.2	1.0981	0.706
133.3	1.1070	0.668
134.3	1.1161	0.630
135.3	1.1191	0.618
135.8	1.1214	0.609
136.3	1.1266	0.587
136.9	1.1422	0.519
137.4	1.1714	0.390
138.2	1.2547	0.023
138.9	1.2604	0.000
139.5	1.2610	
140.5	1.2620	
141.5	1.2628	
144.0	1.2650	
150.2	1.2709	

TABLE XIII  
DILATOMETRY OF SAMPLE 35

<u>Temp .</u> <u>(°C)</u>	<u><math>\bar{V}</math></u> <u>(ml/g)</u>	<u><math>W_c</math></u> <u>—</u>
25.0	1.0421	0.759
40.4	1.0501	0.752
50.0	1.0553	0.747
60.1	1.0613	0.739
70.1	1.0675	0.730
79.6	1.0762	0.709
90.1	1.0868	0.681
99.7	1.0992	0.645
105.6	1.1078	0.619
110.1	1.1140	0.601
114.0	1.1267	0.554
116.0	1.1335	0.528
120.0	1.1457	0.485
123.3	1.1575	0.442
125.9	1.1633	0.423
127.6	1.1671	0.411
129.4	1.1739	0.387
130.2	1.1790	0.367
131.2	1.1844	0.347
132.2	1.1892	0.329
133.3	1.1936	0.313
134.3	1.1994	0.292
135.3	1.2058	0.267
135.8	1.2140	0.234
136.3	1.2251	0.188
136.9	1.2483	0.092
137.4	1.2687	0.007
138.2	1.2711	0.000
138.9	1.2717	
139.5	1.2727	
140.5	1.2733	
141.5	1.2741	
144.0	1.2768	
150.2	1.2834	

TABLE XIV

DILATOMETRY OF SAMPLE 36

<u>Temp.</u> <u>(°C)</u>	<u><math>\bar{V}</math></u> <u>(ml/g)</u>	<u><math>w_c</math></u> <u>—</u>
25.0	1.0538	0.691
50.2	1.0696	0.672
70.9	1.0845	0.649
80.4	1.0946	0.623
90.9	1.1072	0.590
100.5	1.1235	0.539
106.0	1.1322	0.514
109.5	1.1414	0.482
114.7	1.1565	0.430
120.0	1.1761	0.359
123.6	1.1916	0.303
126.7	1.1987	0.282
127.9	1.2011	0.274
129.8	1.2070	0.256
131.2	1.2124	0.238
132.7	1.2186	0.216
133.8	1.2280	0.180
134.8	1.2421	0.125
135.6	1.2599	0.053
136.5	1.2685	0.020
137.2	1.2734	0.003
137.7	1.2743	0.000
138.6	1.2752	
139.1	1.2756	
140.1	1.2766	
142.8	1.2787	
147.1	1.2830	

TABLE XV  
DILATOMETRY OF SAMPLE 37

<u>Temp.</u> <u>(°C)</u>	$\bar{V}$ <u>(ml/g)</u>	$W_c$ —
25.0	1.0656	0.623
50.2	1.0828	0.601
70.9	1.0988	0.577
80.4	1.1109	0.544
90.9	1.1260	0.500
100.5	1.1422	0.452
106.0	1.1539	0.414
109.5	1.1631	0.383
114.7	1.1766	0.338
120.0	1.1931	0.282
123.6	1.2068	0.234
126.7	1.2139	0.213
127.9	1.2158	0.209
129.8	1.2195	0.200
131.2	1.2244	0.183
132.7	1.2302	0.164
133.8	1.2340	0.151
134.8	1.2383	0.137
135.6	1.2410	0.128
136.5	1.2488	0.098
137.2	1.2525	0.085
137.7	1.2593	0.059
138.6	1.2729	0.005
139.1	1.2738	0.003
140.1	1.2754	0.000
142.8	1.2778	
147.1	1.2807	

TABLE XVI

DILATOMETRY OF SAMPLE 38

<u>Temp.</u> <u>(°C)</u>	<u><math>\bar{V}</math></u> <u>(ml/g)</u>	<u><math>W_c</math></u> <u>—</u>
25.0	1.0126	0.930
40.4	1.0174	0.932
50.0	1.0218	0.925
60.1	1.0243	0.930
70.1	1.0281	0.927
79.6	1.0323	0.922
90.1	1.0378	0.912
99.7	1.0440	0.898
105.6	1.0478	0.890
110.1	1.0511	0.881
114.0	1.0541	0.874
116.0	1.0557	0.870
120.0	1.0597	0.858
123.3	1.0634	0.847
125.9	1.0680	0.830
127.6	1.0698	0.825
129.4	1.0744	0.807
130.2	1.0792	0.787
131.2	1.0860	0.758
132.2	1.0927	0.730
133.3	1.0960	0.717
134.3	1.1007	0.698
135.3	1.1066	0.673
135.8	1.1155	0.634
136.3	1.1264	0.587
136.9	1.1656	0.413
137.4	1.2471	0.052
138.2	1.2593	0.000
138.9	1.2599	
139.5	1.2603	
140.5	1.2613	
141.5	1.2622	
144.0	1.2642	
150.2	1.2699	

TABLE XVII

DILATOMETRY OF SAMPLE 39

<u>Temp.</u> <u>(°C)</u>	<u><math>\bar{V}</math></u> <u>(ml/g)</u>	<u><math>w_c</math></u> <u>—</u>
25.0	1.0326	0.814
50.2	1.0429	0.814
70.9	1.0532	0.805
80.4	1.0595	0.795
90.9	1.0674	0.777
100.5	1.0781	0.746
106.0	1.0836	0.732
109.5	1.0890	0.715
114.7	1.0998	0.678
120.0	1.1139	0.627
123.6	1.1249	0.587
126.7	1.1356	0.548
127.9	1.1398	0.533
129.8	1.1546	0.474
131.2	1.1649	0.434
132.7	1.1736	0.401
133.8	1.1815	0.371
134.8	1.1892	0.341
135.6	1.2016	0.291
136.5	1.2398	0.133
137.2	1.2657	0.026
137.7	1.2726	0.001
138.6	1.2732	0.000
139.1	1.2736	
140.1	1.2746	
142.8	1.2769	
147.1	1.2789	

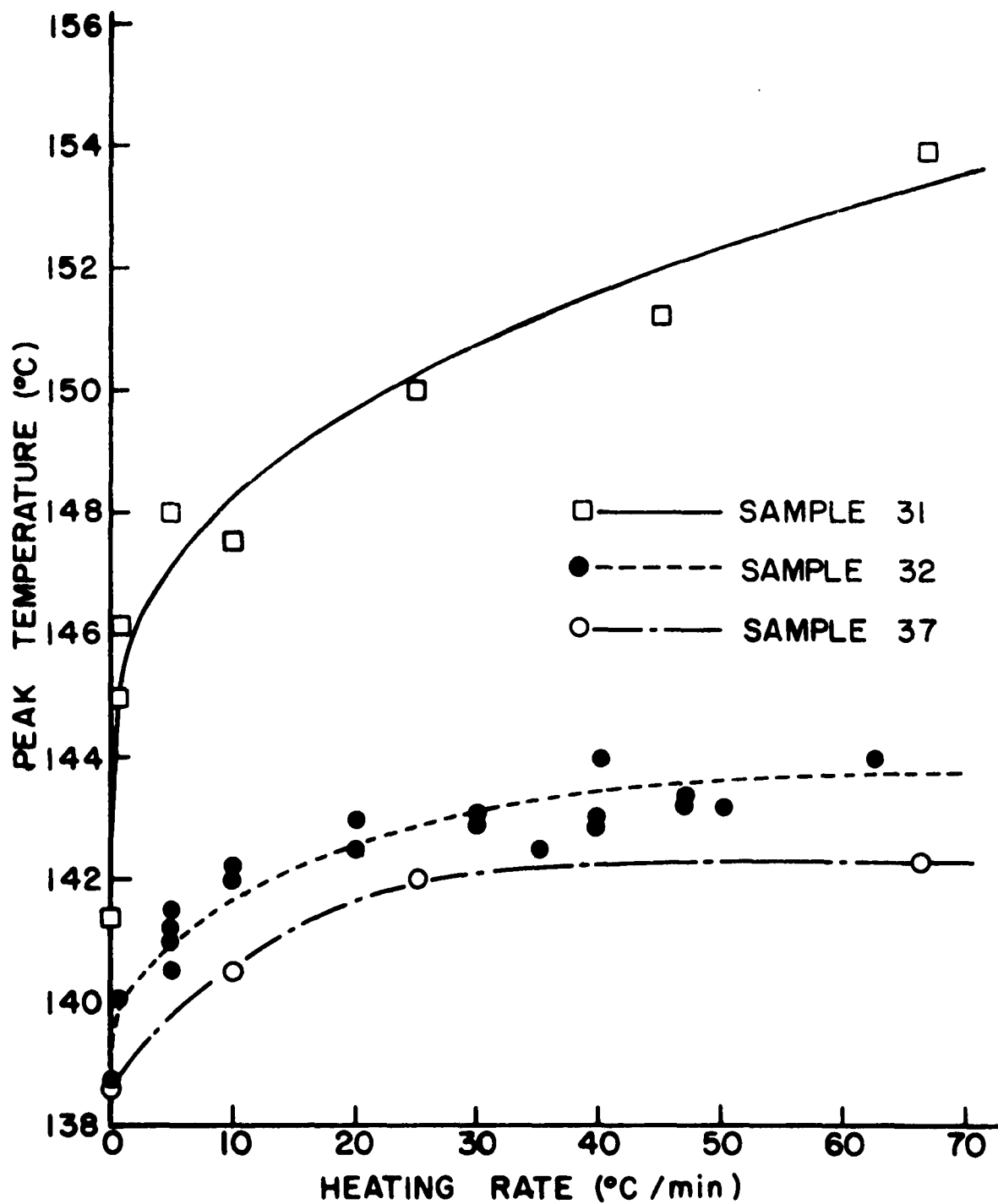


Figure 14. Superheating of extended chain crystals.

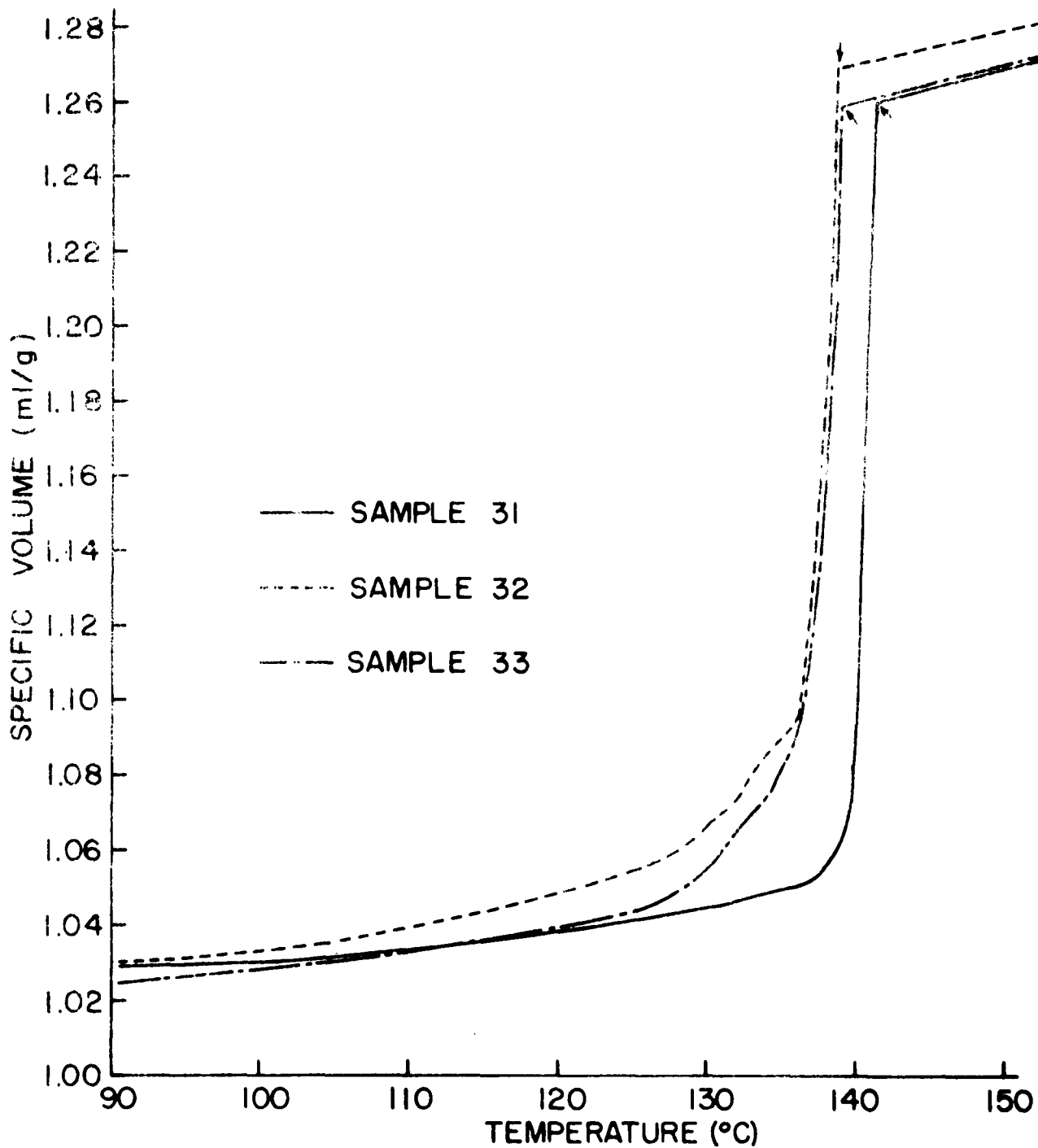


Figure 15. Melting curves of polymethylene and polyethylenes.

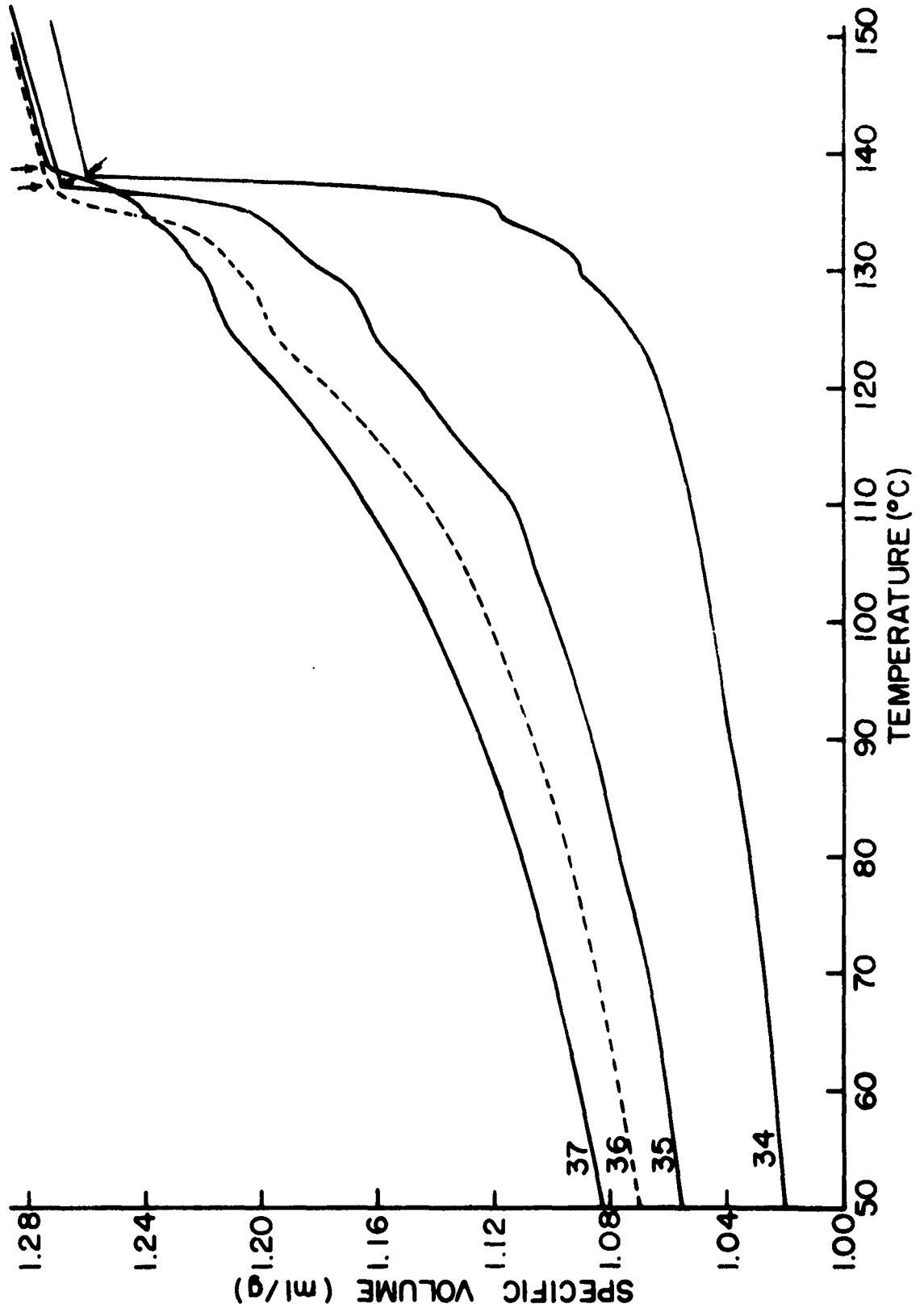


Figure 16. Melting curves for ethylene-butene copolymers.

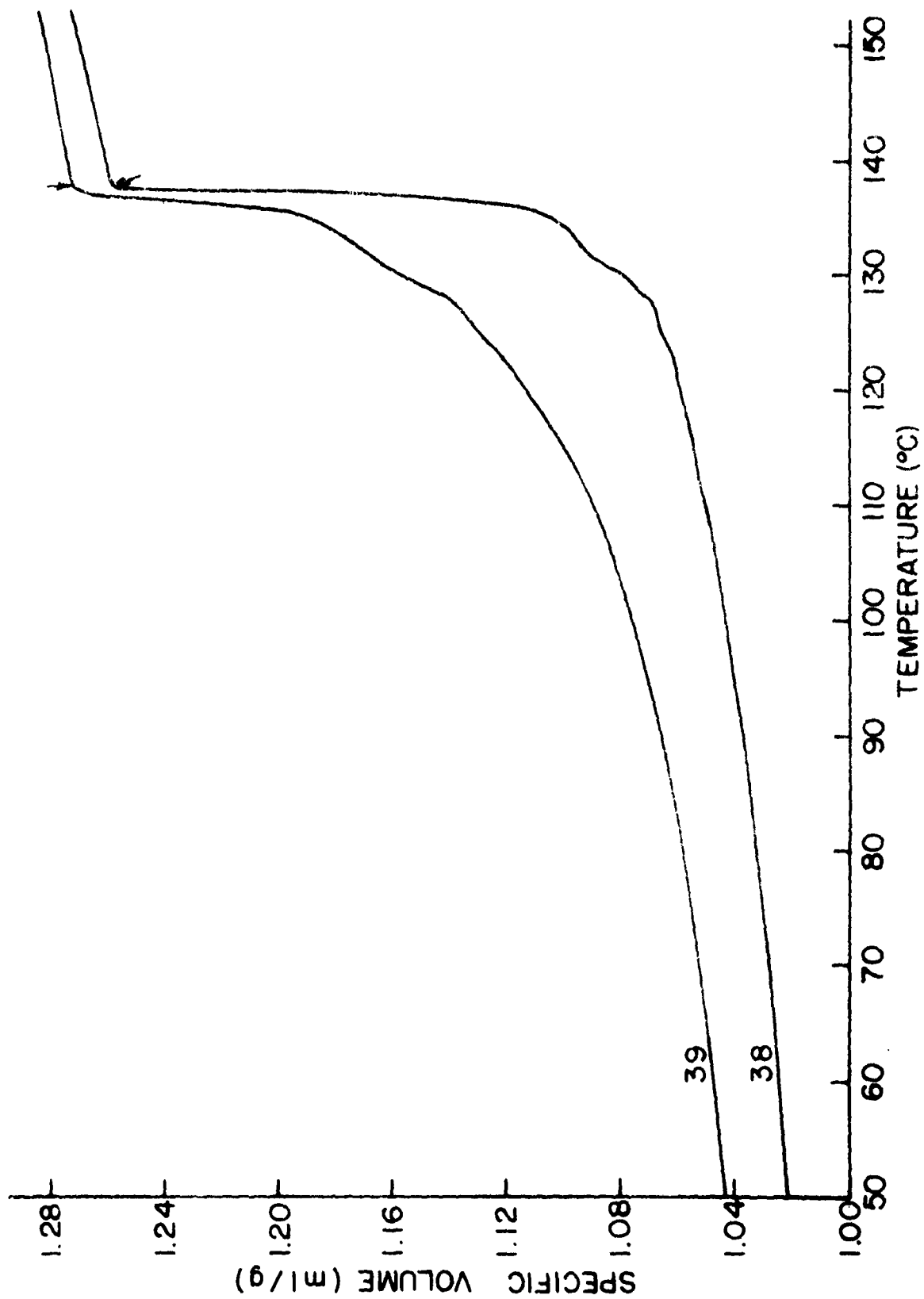


Figure 17. Melting curves for ethylene-propylene copolymers.



Figure 18. Electron micrographs of fracture surfaces of pressure-crystallized polyethylene.

## IV. DISCUSSION

### A. Morphology<sup>39</sup>

The discovery that linear polyethylene crystallizes from solution as lamellar single crystals of folded chain has stimulated reexamination of the traditional fringed micelle model for solid state polymers. It has been recognized that folded chain lamellae are also the basic structures of most linear polymers crystallized from the melt.

Anderson<sup>40,41</sup> studied the morphology of isothermally bulk-crystallized fractions of a linear polyethylene by means of a fracture technique similar to that described in II-F. He observed at least three morphologically distinct lamellar structures in the bulk samples crystallized at atmospheric pressure, which he called types I, II, and III lamellae. Type I (regular lamellae) are similar in appearance to solution-grown folded chain lamellae. Type II (narrow lamellae) consist of ribbon-like layers and have about the same step height as the regular lamellae. However, type II lamellae are limited in width, which is generally slightly more than twice their height. They have been found only in higher molecular weight fractionated samples and are not observed in the whole polymer. The step heights of both type I and II lamellae increase with increasing crystallization temperature. Adequate crystallization or annealing may increase

their step height to 500 to 1000Å.<sup>13,14,42,43</sup> Anderson pointed out that the step height of the type I and II lamellae is equal to the lower of the two low angle spacings observed for bulk-crystallized linear polyethylene.<sup>44</sup>

Type III lamellae were observed for samples with viscosity average molecular weight less than 12,000. Their appearance is similar to that of the bands in polytetrafluoroethylene.<sup>37,38,45</sup> Type III lamellae could be observed both in polyethylene with a broad molecular weight distribution and in low molecular weight fractionated polymer. Anderson has suggested that these lamellae are similar to paraffin crystals, consisting of fully extended chains.

The electron microscopic observation of our samples has revealed that, as crystallization temperature and pressure go higher, type III lamellae increase both in relative proportion and in their maximum thickness until the entire sample is occupied by type III lamellae. The electron diffraction patterns like the one shown in Fig. 12-D demonstrate that the molecules in type III lamellae lie at a right angle to the lamellar or band surfaces. The alignment of the molecules has been shown to be parallel to the striations by observation of the optical birefringence of lamellae attached to the replica.\*

---

\* The optical birefringence was measured by Dr. E. W. Fischer.

Fracture surfaces of highly crystalline samples (samples 14,15, and 31) often show striations nearly perpendicular to the broad faces of the lamellae. These striations are continuous across an entire lamella. As far as the fracture surfaces are concerned, Geil<sup>39</sup> proposed that a type III lamella is made up of sheet-like structures about 300A thick and with large length, their width being equal to the thickness of the lamella. Moreover, these sheets appear to be easily broken into nearly cylindrical structures of several hundred angstroms diameter, their length being equal to the thickness of the corresponding lamella. It would not be justified, however, to assume that the above sheet-like (or rod-like) structures are the fundamental structures of the type III lamellae in pressure-crystallized samples. X-ray low angle patterns, which are expected for either of the structures,<sup>46,47</sup> have not been observed. In addition, type III lamellae with a smooth fracture surface were sometimes observed. These suggest that the sheet-like and the rod-like structures have been created during the process of fracturing. The striations may be characteristic of the fracture surfaces of any thick lamella in which molecules are oriented perpendicular to the broad surfaces of the lamella.

Concerning the incorporation of molecular chains in the type III lamellae of polytetrafluoroethylene, Bunn<sup>37</sup> suggested that the thickness of a lamella was equivalent to the length

of the molecules composing the lamella. However, Speerschneider and Li<sup>38</sup> observed that the average thickness of lamellae in this polymer could be widely changed by changing the cooling rate from the melt. They have also observed that the appearance of the fracture surfaces is not dependent on the lamellar thickness. In the case of our pressure crystallized samples, samples 14 and 15 can well be explained in terms of the "fully extended chain structure" suggested by Bunn<sup>37</sup> and Anderson.<sup>40,41</sup> The average thickness of lamellae of 2500A results in an average molecular weight of 28,000, somewhat larger than those obtained by means of Gel Permeation Chromatography. The thickest lamellae (3 $\mu$ ) correspond to the small portion of the high molecular weight fraction existing in the linear polyethylene. Therefore "fully extended chains" will be the predominant feature of the molecules in samples 14 and 15.

However, fully extended chain structure is not the case for sample 31, for which average chain length (100 $\mu$ ) is far longer than the thickness of the thickest lamellae (6 $\mu$ ). Although the average lamellar thickness of sample 31 is considerably higher than that of a pressure crystallized polyethylene, the density of the latter can often be higher. As the crystalline regions in polymethylene cannot be less ordered than those in polyethylenes, the only explanation is that the areas between lamellae in sample 31 are associated with a considerable amount of amorphous part. Thus the surfaces of

lamellae in sample 31 should not be similar to those of solution-crystallized folded chain single crystals, for which the thickness of the disturbed region is not more than a few angstroms. It is very difficult to expect any kind of coordination between the two end surfaces of a lamella with a thickness of  $6\mu$ . Therefore the behavior of the molecular chain at the surface of the type III lamellae in sample 31 appears to be statistical in nature, as was proposed by Flory.<sup>48</sup>

The comparison of the fracture surfaces of sample 31 and those of sample 14 or 15 shows that the sizable amount of very thin lamellae which always accompany the thick lamellae in the latter samples is rarely observed in the former. This fact also indicates that the thinner lamellae (or lower temperature melting lamellae) in the pressure-crystallized polyethylene are composed of lower molecular weight fractions of the polymer.

Some "fibers" are always observed on the fracture surfaces of type III lamellae. Apparently they have been pulled out of the lamellae during the fracturing process. Comparison of Fig. 12 and Fig. 18 shows that the fibers are related, both in quantity and in length, with the abundance of the molecules whose length exceeds the thickness of the corresponding lamellae.

The fracture surfaces of pressure-crystallized samples often show deformations of type III lamellae such as kinks (Fig. 12-C), rotations, and bowing (Fig. 18-B). Deformations of the type III lamellae in polytetrafluoroethylene have been studied by Speerschneider and Li.<sup>38,45</sup> They showed that stress applied at high temperatures causes noncrystalline modes (sliding and rotation), while at low temperatures the crystalline deformation modes (kinking and bowing) are favored. The deformation in our samples, which are mainly kinks, may have been caused either during the fracture process or by the stress on depressurizing at room temperature after the crystallization.\*

The results of the small angle x-ray diffraction measurements are generally in good agreement with other observations. The observed spacing of 400A for sample 9 corresponds well to the low temperature peak in the DTA trace (peak temperature 133.2°C), as sample 1 with long period 400A shows similar peak temperature. The discrepancy between the long period and the average lamellar thickness observed with the electron microscope (800A) for sample 9 is explained by the existence of a considerable amount of type III lamellae whose thickness is beyond the resolution power of the x-ray camera.

---

\* Recent study by T. Davidson and B. Wunderlich favors the kink formation on depressurization. Their study is based on the comparison of the fracture surfaces of polyethylene and those of asbestos.

## B. Behavior of Polymers under Pressure

There have been few publications on the response of polyethylene to hydrostatic pressure.

The melting of the crystalline phase increases with increasing pressure, satisfying the Clapeyron-Clausius equation,

$$\frac{dT_m}{dP} = \frac{\Delta V}{\Delta S} \quad (5)$$

where  $T_m$  is the melting point of the polymer at pressure  $P$ ,  $\Delta V$  is the volume change on fusion, and  $\Delta S$  is the entropy of fusion. Earlier works by Parks and Richards<sup>17</sup> and Matsuoka<sup>18</sup> gave  $0.02^\circ\text{C}/\text{atm}$  for  $\frac{dT_m}{dP}$  for branched and linear polyethylenes up to 2000atm. Hellwege and co-workers<sup>20</sup> obtained a linear relation between the melting point of a linear polyethylene (Marlex 9) and pressure up to 1500atm with a slope of  $0.025^\circ\text{C}/\text{atm}$ . However, a later report by Matsuoka<sup>20</sup> shows that  $dT_m/dP$  decreases with increasing pressure.  $dT_m/dP$  at 1 atm, 1500atm, and 3000atm are  $0.029$ ,  $0.023$ , and  $0.019^\circ\text{C}/\text{atm}$  respectively.

The amorphous part responds to pressure like a typical liquid. Its compressibility decreases with increasing pressure, while the rate of decrease becomes smaller at higher pressures, showing rapid consumption of the free volume at the early stage of pressurization. At  $203^\circ\text{C}$ , the compressibilities of a linear polyethylene (Marlex 9) are

$14 \times 10^{-5}$ ,  $5.3 \times 10^{-5}$ , and  $3.5 \times 10^{-5}$   $\text{cm}^2/\text{Kg}$  corresponding to the pressures of 1 atm,  $1000 \text{Kg}/\text{cm}^2$ , and  $2000 \text{Kg}/\text{cm}^2$ , respectively.<sup>20</sup>

X-ray measurements on crystalline paraffins have shown that the crystallographic a and b axes of the rhombic cell are more easily compressed, while the c axis does not appreciably change with pressure.<sup>49,50</sup> The compressibility of crystalline polyethylene is approximately  $1.5 \times 10^{-5}$   $\text{cm}^2/\text{Kg}$  at room temperature.<sup>20,49</sup> The over-all effect of temperature and pressure on the specific volume of a linear polyethylene is such that the change of volume by melting decreases with increasing pressure.<sup>21</sup> The specific volumes of amorphous and crystalline polyethylene at 1 and  $1000 \text{atm}$  at  $25^\circ\text{C}$  are given in Table XVIII. The amorphous values have been extrapolated from the measurements above the melting point.<sup>17</sup> The specific volume of the crystalline polyethylene has been calculated from measurements on long chain hydrocarbons.<sup>49</sup>

TABLE XVIII. SPECIFIC VOLUME OF POLYETHYLENE

Sample	Specific Volume at 1 atm (ml/g)	Specific Volume at 2000atm (ml/g)	Difference
Amorphous Polyethylene	1.17	1.07	0.10
Crystalline Polyethylene	1.00	0.97	0.03
Difference	0.17	0.10	

Kabalkina and Troitskaya<sup>49</sup> have reported that at room temperature  $n\text{-C}_{34}\text{H}_{70}$  undergoes an irreversible structural modification from rhombic to triclinic by pressure. The minimum pressure necessary to induce this structural change was reported as 5000Kg/cm. The presence of extra reflections in the x-ray diffraction pattern of polyethylenes, which cannot be explained in terms of the orthorhombic unit cell,<sup>51</sup> have been reported.<sup>52-56</sup> Both triclinic<sup>55</sup> and monoclinic<sup>56</sup> modifications were proposed for the extra nonrhombic unit cell, which is generally produced by elongation or pressing. Theoretical density for these modifications ranges from 0.997 to 1.00g/ml, which is similar to that of orthorhombic structure determined by Bunn.<sup>51</sup> Recently Powers and Van Valkenburg<sup>57</sup> have reported an irreversible structural change of polyethylene from rhombic to pseudotriclinic by pressurizing a sample between diamond anvils up to 70°K:bars. Generally these nonrhombic unit cells of polyethylene are associated with a strong reflection at 4.56A, which is the same as the amorphous peak position. This coincidence has been blamed as a cause of error for crystallinity determination by x-ray.<sup>58,59</sup>

Our measurement on pressure-crystallized polyethylene showed that (110) and (200) peak positions are fixed at 4.12 and 3.72A, respectively, for crystallization pressure up to 5200atm (see Table V). Moreover, the diffuse peak at 4.56A

becomes vanishingly small for highly crystalline materials, and the crystallinity by x-ray, assuming the peak at 4.56A to be amorphous, was found to be in good agreement with the density crystallinity for all samples (see Fig. 11). These results suggest that hydrostatic pressure does not cause an irreversible change of the orthorhombic unit cell structure of polyethylene. The change may only be caused by sheer stress as by elongation and inhomogeneous pressure (pressing). This view is consistent with the fact that the theoretical densities of the nonorthorhombic modifications hitherto reported are not higher than that of the orthorhombic modification.

Few data are available for the viscosity of polyethylenes at high pressures. Westover<sup>60</sup> measured the bulk viscosity of polyethylenes over a range of hydrostatic pressure up to 25,000 psi and temperature up to 250°C. He has noticed that linear polyethylenes are less pressure sensitive with regard to viscosity than more branched polyethylene and that the higher molecular weight polyethylenes increase more in viscosity with pressure than do the lower molecular weight polyethylene.

Generally, when the logarithm of the viscosity is plotted against pressure, it is initially concave towards the pressure axis, approaching a straight line at intermediate pressures and finally becoming convex towards the pressure axis.<sup>61</sup> At

250°C the viscosity of a linear polyethylene at 1700atm has been observed to be about seven times as high as that at 140atm.<sup>60</sup> The dependence of viscosity on pressure over this pressure range seems to correspond to the "initial stage."

The effect of pressure on the crystallization rate can be divided into the effect on the nucleation process and that on the growth rate. The steady state nucleation rate can be expressed as<sup>62</sup>

$$\frac{dN}{dt} = N_0 e^{-\frac{E_D}{RT}} \cdot e^{-\frac{\Delta F^*}{RT}} \quad (6)$$

where  $N_0$  is a frequency factor,  $E_D$  the activation energy of diffusion, and  $\Delta F^*$  the Gibbs free energy of formation of the critical nucleus. The growth rate will be determined by the long range diffusion of the crystallizable sequences. Though the pressure can change both  $E_D$  and  $\Delta F^*$ , the main effect is expected to be through the increase in  $E_D$  by pressure. More information on the relations between viscosity, pressure, and temperature is required.

### C. Crystallization of Linear Polyethylenes at High Pressure<sup>63</sup>

Figures 6, 9, and 10 show that two different types of crystals are grown depending on temperature and pressure. Based on the dependence of melting behavior and density on pressure, we divide the discussion into three parts, covering the crystals grown below 2000atm, above 3500atm, and in the intermediate region.

Polyethylene Crystallized below 2000atm

In this region a small increase in the density of the samples at atmospheric pressure was observed. The increment is almost proportional to the pressure and is about 0.006g/ml at 2000atm (see Fig. 10). Little difference was observed between the crystallization at a constant degree of supercooling (samples 1-6) and the crystallization at constant cooling rate (samples 16-19). An increase in melting point was observed to go parallel with the increase in density. Figure 9 shows an increase of about 1.5°C in the experimental maximum melting point. DTA traces of all samples in this region show only one peak, indicating no morphological change by pressure. All these observations support the hypothesis that the samples consist of thin lamellar crystals, the thickness of which increases with increasing crystallization pressure as was observed in the case of crystallizations of the same polymer from solution under elevated pressure.<sup>64</sup> This has been proved by the electron microscopic investigation of fracture surfaces (see IV-A).

The result of low angle x-ray measurement shows that the average thickness of lamellae increases from 400A for sample 1 to 600A for sample 6. Assuming that no reorganization of lamellar structure takes place on heating, a thickness increase from 400A to 600A corresponds to a decrease in specific surface

area of  $1.7 \times 10^5 \text{ cm}^2/\text{g}$ , which can account for the increase in melting point. Brown and Eby<sup>65</sup> carried out the measurements of lamellar thickness (electron microscopy), low angle x-ray spacings, melting temperature, and density for linear polyethylene samples crystallized at pressures up to 1000atm. Although the melting points they obtained are a little higher than ours, the results are generally in good agreement with ours. Although they could observe only one type of lamellae in the fracture surfaces, their small angle measurements suggest the existence of two kinds of structures, one of which may be connected with a paraffin-like structure.

The difference between the samples grown at a constant degree of supercooling and those crystallized by cooling the melt from 170°C at the rate of 4°C/hr is slight in all respects, which means that crystallization occurred at about the same temperature in both cases. This means that 170°C is above the crystallization temperature of the polymer up to 2000atm.

#### Polyethylene Crystallized above 3500atm

Linear polyethylene samples crystallized in this pressure range have quite different properties from those of those samples crystallized at lower pressures. They are generally very brittle and can be fractured easily at room temperature. A density crystallinity as high as 99% was achieved (sample 33).

Wide angle x-ray diffraction patterns show sharper peaks for (200) and (110) spacings, indicating the presence of well developed crystallites.

As is shown in Fig. 9, the experimental maximum melting point is much higher for the sample crystallized in this pressure range and reaches a plateau of  $140 \pm 0.5^\circ\text{C}$  at about 4000atm.

DTA traces of these highly crystalline samples have one or more low temperature peaks. Low angle x-ray measurement, however, showed no discrete or diffuse scatter below  $600\text{\AA}$ , the limit of the instrument. This would seem to indicate that these small low temperature peaks are not necessarily residual folded lamellae. As is shown in Fig. 8, the low temperature peaks shift to still lower temperatures by the recrystallization under quenching conditions. However, they cannot be shifted easily to higher temperatures by annealing. Moreover, melting and reorganization of one of the low temperature peaks does not affect the melting behavior of the peaks at higher temperatures (Fig. 8). Therefore the crystalline areas which are responsible for the different peaks appear to be independent of each other. These observations along with the absence of low temperature peaks for sample 31, indicate that the small low temperature peaks in highly crystalline polyethylenes are connected with low molecular weight fraction of the samples. Calorimetric measurement of

sample 33 shows that low temperature peaks account for 17% of the total heat of fusion. It means that if the above assumption is correct, molecules shorter than 360A (MW 4000) will be rejected by the crystalline regions corresponding to the high temperature peak of sample 33.

The samples crystallized at high pressure but at high degrees of supercooling often show high temperature peaks (samples 23-26). The poor reproducibility suggests, however, that the crystallization under this condition takes place during the initial pressurization. Broader high temperature peaks of samples 23 and 25 indicate that the crystallites in these samples have a wide size distribution and that the amount of extended chain crystals is less than in sample 14. This is also demonstrated by the lower densities of samples 23-26 compared to samples 12-15.

#### Intermediate Region (2000-3500atm)

Crystallization in this pressure range is characterized by a transition from the formation of folded chain crystals to extended chain crystals. Density at atmospheric pressure first drops as pressure increases, reaches a minimum value comparable with that of the same polymer crystallized at atmospheric pressure at a similar degree of supercooling, and then increases again (fig. 10). The experimental maximum melting point also shows an initial drop (Fig. 9). However,

in the middle of this pressure range, DTA traces show the appearance of a high temperature shoulder which eventually develops into a high temperature peak (Fig. 6). Matsuoka<sup>66</sup> reported that in the case of a linear polyethylene (Marlex 50), an increase of crystallization pressure from 1200atm to 2600atm at 160°C resulted in a decrease of density by 0.013g/ml. This is in good agreement with our measurements on samples 18-22.

The transition from folded chain to extended chain structure was also confirmed by electron microscopy. DTA traces and small angle x-rays show that in this intermediate region folded chain lamellar type crystallites decrease both in quantity and in thickness.

The above arguments concerning the separate regions will be combined to form the conclusion that the formations of folded chain crystals and extended chain crystals are two competitive processes with different mechanisms. Under atmospheric pressure and at a certain degree of supercooling the folded chain mechanism is kinetically favored for longer molecules. Only low molecular weight fraction can crystallize into extended chain structure under these circumstances. Application of pressure up to 2000atm, keeping the degree of supercooling constant, increases lamellar thickness slightly but does not change the relative rates of the two processes

extensively. At above 2000atm, however, the rate of the former process decreases while the latter process becomes increasingly favored with increasing pressure, until finally at 3500atm the formation of extended chain structure is the dominant process of crystallization. At above 2500atm, both processes are rather slow, and the crystallinity takes a minimum value.

Although a direct measurement of the rate of crystallization was not intended in our experiments, there have been some indications that the formation of extended chain structure at high pressure proceeds at a high rate. For instance, when an initial pressure of 4800atm was applied to a linear polyethylene at 227°C (sample 32), a gradual decrease of pressure followed, which reminded one of decrease of specific volume at isothermal crystallization of linear polymers.<sup>67</sup> The major part of the pressure decrease, amounting to 120atm, occurred in 15 minutes. Assuming a compressibility of  $10^{-5} \text{atm}^{-1}$  for the oil, and 200ml for the high pressure system, this decrease in pressure corresponds to a volume decrease of 0.24ml on the side of the sample, which is a proper magnitude for the crystallization of 15g of polyethylene under this condition.

Because of the difficulty of rearranging very long polymer molecules, the highest melting point yet reported for polymethylene (uninhibited) has been  $136.5 \pm 0.5^\circ\text{C}$ .<sup>68</sup> For the same

reason, Matsuoka and Aloisio<sup>69</sup> obtained a low crystallinity of 67% for a high molecular weight linear polyethylene (MW > 10<sup>6</sup>). In the light of these observations, the high crystallinity (97%) and melting point (141.4°C) of sample 31 demonstrate the remarkable effect of high pressure and temperature on the rate of crystallization of linear polymers.

The crystallizations of linear polyethylene at 170°C and at various pressures (samples 6 and 16-26), and those at a constant pressure and at different temperatures (samples 27-30) indicates that pressure is a more critical factor than temperature in deciding the mode of crystallization.

#### D. Melting of Polyethylenes and Polymethylene with Extended Chain Structure

The nature of a flexible linear polymer above the melting point is characterized by random conformations of the molecules. Continuous change into different conformations takes place by more or less hindered rotation around the backbone chain bonds. When the melt is cooled, crystalline regions may appear. In the crystalline state, free rotation around single bonds is impossible. The randomness of molecular conformation in the melt is, however, more or less retained in the semicrystalline state. One extreme case of partial crystallization is the nonequilibrium limit of cold crystallization discussed by Wunderlich,<sup>70</sup> where only minimal ordering of

molecules takes place on crystallization. This situation can be realized for polymers which can be quenched from the melt below their glass transition temperatures without any crystallization. By subsequent annealing at temperatures little above the glass transition temperature, cold crystallization can be achieved.

However, when linear polymers are cooled from the melt under normal conditions, the formation of spherulites is the characteristic mode of crystallization. A spherulite is a complex aggregate of lamellar structures originating from a nucleus.<sup>8</sup> Polymer molecules are observed to be perpendicular to the lamellae with chain foldings. The thickness of the lamellae in spherulites depends on the degree of supercooling at the crystallization, higher degrees of supercooling resulting in thinner lamellae. Spherulites, like solution grown folded chain single crystals and dendrites, are metastable crystals.

Wunderlich<sup>71</sup> introduced a "path of zero entropy production" as the means of determining the "melting point" of metastable crystals. Entropy production in a system may arise from recrystallization and rearrangement of defect concentrations as well as from superheating. In order to realize a path of zero entropy production, a heating rate has to be adopted which is faster than the rate of reorganization or

recrystallization in a metastable sample, but slow enough not to cause superheating.

It has been demonstrated that a heating rate which is ten times faster than the cooling rate during crystallization is the approximate path of zero entropy production for melt-crystallized polyethylene samples.<sup>25,72-75</sup> A heating rate faster than 15°C/min was shown to be appropriate for solution-grown folded chain lamellae of linear polyethylene with thicknesses of  $144 \pm 13 \text{ \AA}$ .<sup>76</sup>

There have been no previous reports on the superheating of linear high polymer crystals. As a matter of fact, it is almost impossible to cause superheating on folded chain polyethylene single crystals grown from solution.<sup>76</sup> The dependence of the DTA peak temperatures on the heating rate, as is shown in Fig. 8, indicates superheating of the extended chain lamellae in these samples. In the case of sample 32, a DTA trace (heating rate 1.5°C/min) shows a time interval of 100 seconds between the recording of equilibrium melting point (138.7°C) as found by dilatometry and that of the disappearance of the last traces of crystallinity (141.1°C). This will roughly correspond to saying that the largest lamellae in the sample can stand surroundings with a temperature 1°C higher than their equilibrium melting point for more than a minute. When a lamella with a thickness of  $2d$  (cm) at its equilibrium melting

point ( $T_m$ ) is dipped in a heat bath at  $T$  ( $T > T_m$ ), the time taken for the center of the specimen to reach the temperature of superheat is at most<sup>83,84</sup>

$$t = Hd/K(T-T_m) \quad (7)$$

where  $K$  is the mean thermal conductivity over this temperature range and is at least  $5 \times 10^{-4}$  cal/°K cm-sec for a linear polyethylene.<sup>85</sup>  $H$  is the sum of the heat of fusion and the integrated heat capacity within this temperature range for the sample of  $d$  ( $\text{cm}^3$ ). For a polyethylene lamella having a thickness of  $3\mu$  and at  $T$  ( $T = T_m + 1$ ),  $t$  is approximately  $3 \times 10^{-3}$  sec. Comparing this with experimental results, we can conclude that superheating was achieved during the DTA measurement. This is the first case of superheating for any crystal of linear high polymer.

Superheating has been demonstrated on some crystals.<sup>77-84</sup> All observations reported so far show that melting starts at the surface of a crystal and proceeds inwards. If the velocity of this process, designated by  $\mu$ , is small compared with the thermal conductivity,  $K$ , of the boundary region of the melt and the crystal, superheating may take place.<sup>84,86</sup> Phenomenologically small value of  $\mu/K$  is often satisfied by crystals, the melt of which is highly viscous.<sup>84</sup> This condition of high viscosity is well satisfied by any crystals of high molecular weight polymers. Therefore the slow melting

rate of our samples has to be connected with a special mechanism of melting of extended chain structure. This view is supported by a report of superheating of polytetrafluoroethylene,<sup>76</sup> which is well known for its extended chain structure. Although the mechanism of melting of extended chain crystals is still to be elucidated, a probable rate determining step may be the relaxation of an extended chain into a random coil on melting. Thus a great extent of superheating will be realized for a polymer crystal with larger dimensions in all directions, higher molecular weight, and lesser amounts of inner defects. Polymethylene (sample 31), which satisfies all these criteria best of all, showed superheating as high as 12°C.

It is thus clear that the correct measurement of the melting point of extended chain lamellae is possible only through very slow heating rate. Dilatometry, which is the most suitable tool for this purpose, gave a melting point of 141.4°C (414.6°K) for polymethylene, the highest yet recorded for polyethylene and polymethylene. It also gave the linear polyethylenes (A and P<sub>1</sub>) a sharp melting point at 138.7°C.

The equilibrium melting temperature  $T_m^0$ , the melting temperature of the "hypothetical" perfect crystal of linear polyethylene, has been a matter of great concern. Experimentally, a most careful measurement by Chiang and Flory<sup>87</sup>

gave a melting point of 138.5°C for a high molecular weight fraction of linear polyethylene (Marlex 50). The low angle x-ray spacing of this sample was reported to be approximately 1100Å.

In order to avoid the kinetic limitation for the crystallization at low supercooling, extrapolation from the measurements on n-paraffin hydrocarbons has often been employed to determine the value of  $T_m^0$ . Broadhurst<sup>88</sup> obtained 141.1±2.4 (°C) for  $T_m^0$  by empirical extrapolation of the melting points of n-C<sub>n</sub>H<sub>2n+2</sub> with n above 44.

Flory and Vrij<sup>89</sup> introduced a term  $R/n$  into the molar entropy of fusion of n-C<sub>n</sub>H<sub>2n+2</sub>. The correction based on this term gave  $T_m^0$  of 145.5±1°C for the same data as Broadhurst. Hoffman and Weeks<sup>90</sup> reported a linear relation between the observed melting point ( $T_m'$ ) and crystallization temperature ( $T_x$ ).  $T_m^0$  is expected to be obtained from the intersection between the extrapolation of this relation and  $T_x = T_m'$ . They arrived at a value of 143±2°C for  $T_m^0$  of polyethylene. These values for  $T_m$  obtained by extrapolation are fairly close to our experimental melting point of polymethylene.

A rather large difference between the dilatometric melting points of linear polyethylene (samples 32 and 33) and polymethylene (sample 31) can probably be attributed to their different molecular structures and molecular weight distributions, as the effect of lamellar thickness is negligible

for crystals with a thickness on the order of  $1\mu$ . According to Bryant,<sup>91</sup> Marlex 50 type polyethylene contains 0.09-0.06 side chains per hundred chain carbon atoms. Low pressure polyethylene is also known to contain side chains.<sup>92</sup> Therefore the mole fraction of crystallizable units,  $X_{CH_2}$ , for our linear polyethylene is expected to be about 0.995 (see Table III). A simple thermodynamic treatment of the effect of noncrystallizable units on the chemical potential of crystallizable units in the melt leads to an expression for melting point depression,<sup>94</sup>

$$\Delta T = \frac{R(T_m)^2}{\Delta H} (1 - X_{CH_2}) \quad (8)$$

where  $T_m$  is the melting point when  $X_{CH_2}$  is unity. For polyethylene,  $\Delta H = 920\text{cal}$ .<sup>35</sup> For  $X_{CH_2} = 0.995$ ,  $\Delta T$  turns out to be  $1.9^\circ\text{C}$ . The effect of side chains on the melting point is negligible (see section IV-E).

This estimation is smaller than the actual melting point depression of  $2.7^\circ\text{C}$ . Chiang and Flory<sup>87</sup> reported, however, that elimination of low molecular weight fraction increased the melting point of Marlex 50 far more than was expected from Eq. (8). This discrepancy will be avoided if we consider the equilibrium between segments, which may consist of several crystallizable units, rather than that between crystallizable units. In the case of polymethylene (sample 31),

both our knowledge of molecular structure and molecular weight distribution and the electron microscope study show no reason for melting point depression. Therefore 141.4°C must be very close to the equilibrium melting point of infinitely long linear polyethylene or polymethylene.

Once we have established the equilibrium melting point  $T_m^0$ , we can estimate the surface free energy of lamellae using the equation<sup>93</sup>

$$T_m = T_m^0 \left( 1 - \frac{2\sigma_e}{\Delta h_f \cdot l} \right) \quad (9)$$

where  $T_m$  is the average melting point of lamellae and is close to DTA peak temperature.  $l$  is the average lamellar thickness and corresponds to the small angle x-ray spacing of the sample.  $\Delta h_f$  is the heat of fusion of 1 ml of crystals and is 66 cal for polyethylene.<sup>35</sup> The results of the surface energy calculation are listed in Table XIX. Table XIX also contains two additional measurements on single crystals of the same polymer grown from solution (SC-1 and SC-2). Similar values of surface free energy for all the samples indicate that the surface structure of type I lamellae in polyethylene crystallized from the melt is closely related to that of folded chain lamellar single crystals grown from solution.

TABLE XIX. SURFACE FREE ENERGY OF POLYETHYLENE LAMELLAE  
CRYSTALLIZED FROM MELT AND SOLUTION

Sample	Mode of crystallization	$T_m$ (°C)	$l$ (Å)	$\sigma_e$ (erg/cm <sup>2</sup> )
1,2	130°C from melt	133.7	400	84
6	170°C from melt	135.2	600	97
9	186°C from melt	133.2	400	91
SC-1	80°C and 100°C from solution	118.0	130	96
SC-2	90°C from solution	122.1	146	88

#### E. Melting of Polyethylene Copolymers with Extended Chain Structure

Flory<sup>94</sup> has developed an equilibrium theory of crystallization and melting of copolymers. His model copolymer consists of sequences of A units of various lengths connected by intervening B units. B units are assumed to be rejected by the crystal lattice of A units and therefore to be non-crystallizable.

The basic assumptions employed are.

(a) The size of a crystallite in the chain direction expressed by  $\xi$ , the number of A units of a given chain that traverses the crystallite from one end to the other, is restricted by the occurrence of B units along the polymer chains.

(b) The lateral development of a crystal length is limited by the availability of A sequences in the melt which are at least  $\zeta$  in length.

(c) The melt composition will be established by the statistical equilibrium between A sequences in the crystalline region and those in the melt.

(d) The temperature at which a crystallite melts depends upon its thickness  $\zeta$  through end surface energy and upon the chemical potential of A sequences of length  $\zeta$  in the adjoining melt phase.

Based on the above assumptions, physico-chemical calculations lead to two important results.

First, the equilibrium melting temperature of a copolymer,  $T_m$ , is given by

$$\frac{1}{T_m} - \frac{1}{T_m^0} = - \frac{R}{\Delta H_u} \ln p \quad (10)$$

where  $T_m^0$  is the equilibrium melting point of the homopolymer of A units,  $\Delta H_u$  the heat of fusion per mole of A units, and  $p$  the sequence perpetuation probability. For a random copolymer  $p$  is equal to the mole fraction of A units,  $X_A$ , in the copolymer.

Secondly, the equilibrium crystallinity as a function of temperature and polymer composition is given as

$$w_c = \frac{X_A}{p} (1-p)^2 p^{\zeta^*} \left\{ p(1-p)^{-2} - e^{-\theta} (1-e^{-\theta})^{-2} + \zeta^* [(1-p)^{-1} - (1-e^{-\theta})^{-1}] \right\} \quad (11)$$

where  $\zeta^*$  is the minimum length of A sequences which can crystallize under the present conditions.  $\zeta^*$  depends on P,  $\Delta H_u$  and end surface free energy.  $\theta$  is a temperature scale defined by

$$\theta = (\Delta H_u / R) (1/T - 1/T_m^0) \quad (12)$$

Equation (10) predicts depression of the melting of a homopolymer by the introduction of noncrystallizable units along the polymer chains. Gradual disappearance of the crystallinity of copolymers over a broad temperature range is expected from Eq. (11). Both equations were shown to be in qualitative agreement only with experimental results.<sup>67</sup>

The melting curves of samples 34 through 39 (Figs. 16 and 17) show that methyl and ethyl side groups reduce the crystallinity of the pressure crystallized samples and make their melting range broader. As is shown in Fig. 19, the crystallinity decreases linearly with increasing concentration of foreign groups. One can calculate that every foreign group in the samples decreases the crystallinity by 27 CH<sub>2</sub> groups. The same magnitude of effect was reported by Bodily and Wunderlich<sup>26,75</sup> for ethyl side groups in ethylene-butene copolymers crystallized at atmospheric pressure. Their results are shown by filled circles in Fig. 19.

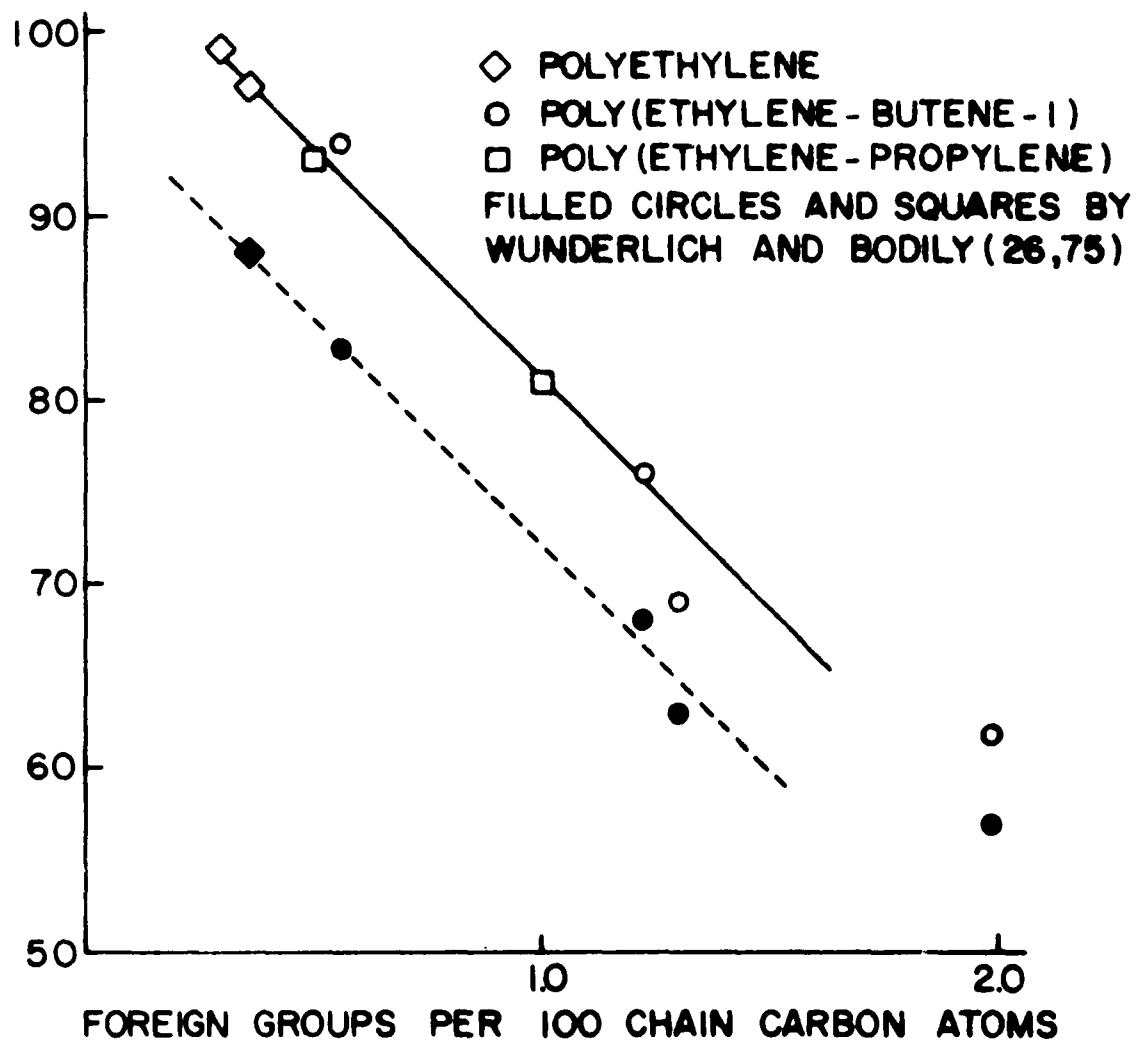


Figure 19. Crystallinity by density of polyethylene copolymers crystallized at high pressure.

Figure 20 demonstrates the dependence of the melting point by dilatometry on the concentration of foreign groups. The solid line is the theoretical melting point calculated from Eqs. (8) and (10). It should be pointed out that the theoretical melting point depression by end groups is almost the same for all the polymers (except polymethylene), as they have similar number average molecular weight (ca.  $10^4$ ). The melting point of the same polymers when crystallized from the melt at atmospheric pressure is shown in the figure by filled circles. An amazing thing about Fig. 20 is that the melting points of these pressure-crystallized copolymers are independent of the concentration of the side groups. The theoretical curve, which is qualitatively satisfied by the polymers crystallized at atmospheric pressure, does not hold for the pressure-crystallized samples. The considerable difference between the melting point of polymethylene and those of the rest of the polymers is probably due to molecular weight distributions of the polymers. The considerable amount of low molecular weight fraction which is contained in all the polymers except polymethylene seems to be responsible for the depression of the melting point. (See Figs. 4 and 5 and section IV-D.)

The fact that methyl and ethyl side chains have little effect on the melting point suggests the formation of solid solution, i.e., both ethyl and methyl groups can be incorporated

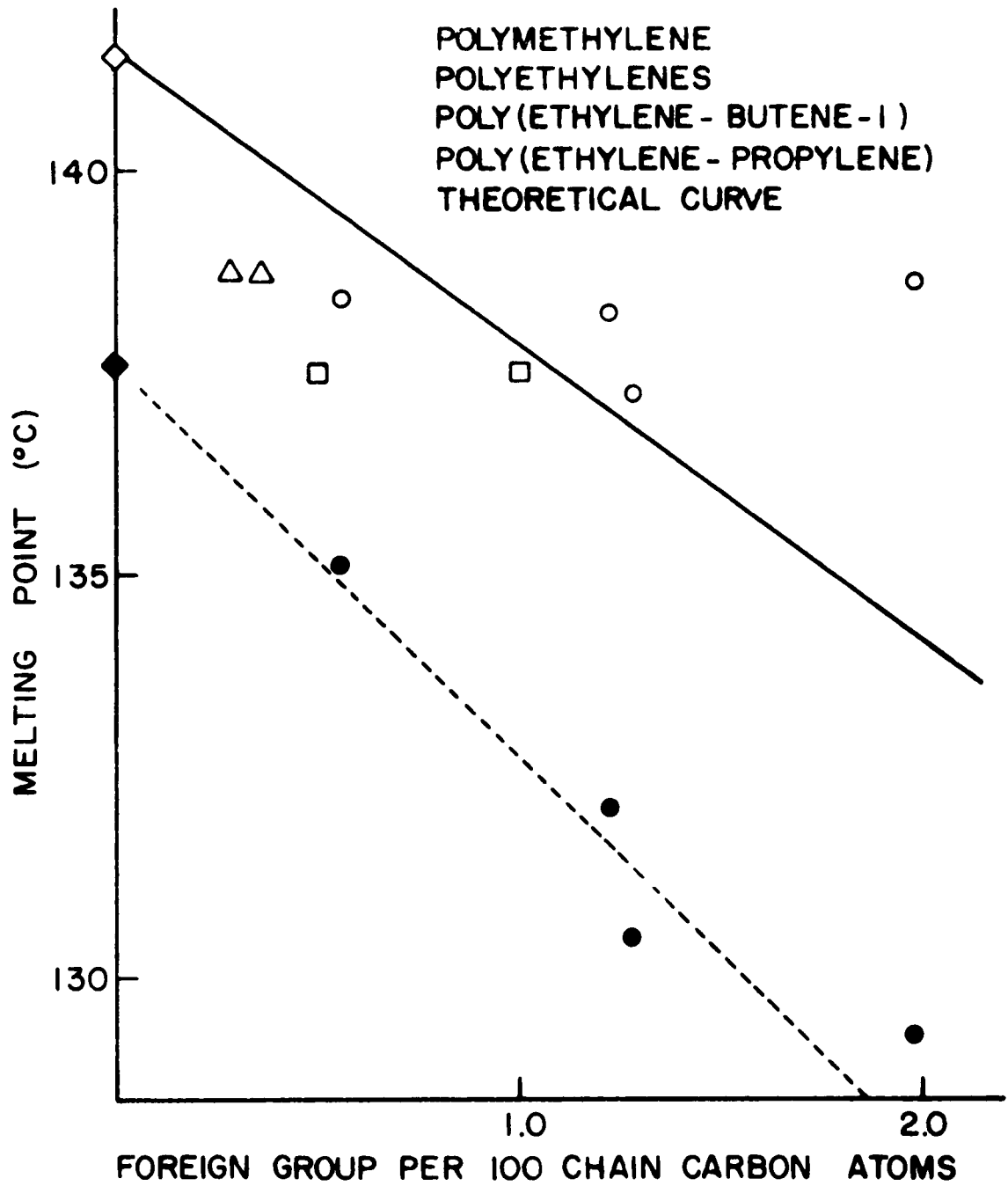


Figure 20. Melting points of polyethylene copolymers crystallized at high pressure.

in the crystalline phase at equilibrium. Flory and co-workers<sup>32</sup> have reported that when copolymers of polymethylene are crystallized very carefully a small amount of methyl side chains (less than one per 100 chain carbon atoms) does not change the melting point of the sample, while propyl and ethyl branchings are apparently excluded from the crystalline phase.

There have been many reports based on x-ray measurements that copolymer groups are not completely rejected out of crystalline regions. Walter and Reding<sup>95</sup> found a variation of theoretical crystalline fraction density of from 0.956g/ml (for highly branches polyethylene) to 1.014g/ml (for linear polyethylene) caused mainly by variations of a and b unit cell dimensions. Eichhorn<sup>96</sup> carried out similar measurements on ethylene-propylene copolymers. He found a uniform increase in (110) spacing with increasing propylene percentage. Slight line broadening was also observed, which indicates a decrease in crystallite size and an increase in lattice strain. Cole and Holmes<sup>33</sup> and Swan<sup>97</sup> confirmed the same effect working with alkyl branches up to five carbons in length. They have reported that the main change of unit cell dimensions is in the direction of the a-axis. Cole and Holmes<sup>33</sup> found the effect of methyl, ethyl, propyl and butyl groups on unit cell dimensions to be virtually equal. The only difference between

these groups is in the power of destroying crystalline regions. Similar results have been reported by Wunderlich and co-workers<sup>25,26,75</sup> for a variety of polyethylene copolymers.

All these experiments indicate that side chains, like short alkyl groups, can be accommodated to a certain extent in the crystalline unit cell of polyethylene. In the process of incorporating side chains in the crystal lattice, a kinetic limitation can be expected. Such a kinetic reason might explain the apparent rejection of large alkyl side chains by the crystalline region of polymethylene copolymers which was observed by Flory and co-workers.<sup>32</sup> Application of high pressure during crystallization seems to reduce such a kinetic limitation.

As Table VII shows, the melting points of samples 34 to 39 by DTA are one to two degrees higher than those obtained by dilatometry, indicating that very thick crystals, probably of extended chain structure, have been formed in these samples. A more detailed dependence of DTA peak temperature on the heating rate is given in Fig. 14 for sample 37.

DTA traces of samples 34-37 (Fig. 13) have more complex structures than those of pressure-crystallized polyethylenes. As the concentration of side chains increases, the area under the high temperature peak decreases until the greater

portion of the crystalline part belongs to the lower temperature peaks (sample 37). These lower temperature peaks were observed to remain at the same position despite the various heating rates. This implies that they correspond to folded chain lamellae.

It can be stated, therefore, that the formation of extended chain crystals and that of folded chain lamellae are also two competing modes of crystallization in the polyethylene copolymers. Although the former process is apparently favored at high pressure and high temperature, it is made increasingly difficult by the introduction of side groups. As a matter of fact, no high temperature peak was observed for a branched polyethylene (3.3 side groups per 100 chain carbon atoms) which crystallized at 196°C and 4800atm for 8 hours, followed by cooling to room temperature at the rate of 4°C/hr. It has been reported that the melt viscosity of polyethylene at high pressure is increased by the introduction of side chains. Therefore introduction of side groups disfavors the formation of extended chain crystals, which require long range diffusion of molecules, more than it disfavors that of folded chain crystals.

It is thus clear that Eqs. (10) and (11) do not hold for polyethylene copolymers with methyl and ethyl side chains crystallized at high pressure. Furthermore, the above arguments claim that the wide melting temperature range and the

melting point depression, which have been regarded as equilibrium properties of copolymers, can often be kinetic in nature. Further work using better characterized polymers is desirable in order to elucidate the nature of the melting of copolymers and to establish the limits of the formation of solid solutions of polyethylene.

## REFERENCES

1. Bragg, W. L., The Crystalline State, Vol. I, G. Bell and Sons, London, 1933,
2. Scherrer, P., Gottinger Nachrichten 2, 98 (1918).
3. Herrman, K., O. Gerngross and W. Abitz, Z. physik. Chem. B-10, 371 (1930); Herrman, K. and O. Gerngross, Kautchuk 8, 181 (1932); and Hess, K. and H. Kiessig, Z. physik. Chem. 193, 196 (1944).
4. Flory, P. J., Principles of Polymer Chemistry, Cornell University Press, Ithaca, New York, 1953.
5. Till, P. H., J. Polymer Sci. 24, 301 (1957).
6. Keller, A., Phil. Mag. 2, 1171 (1957).
7. Fischer, E. W., Z. Naturforsch. 12a, 753 (1957).
8. Geil, P. H., Polymer Single Crystals, Interscience Publishers, New York, 1963.
9. Geil, P. H., J. Appl. Phys. 33, 642 (1962).
10. Magil, J. H. and P. H. Harris, Polymer 3, 252 (1962).
11. Symons, N. K. J., J. Polymer Sci. A-1, 2843 (1963).
12. Bunn, C. W. and D. R. Holmes, Trans. Faraday Soc. 25, 95 (1958).
13. Mandelkern, L., A. S. Posner, A. F. Diorio and D. E. Roberts, J. Appl. Phys. 32, 1509 (1961).
14. Pollack, S. S., W. H. Robinson, R. Chiang and P. J. Flory, J. Appl. Phys. 33, 237 (1962).

15. Wood, L. A., N. Bekkedahl, and R. E. Gibson, J. Chem. Phys. 13, 475 (1945); McGeer, P. L. and H. C. Duus, J. Chem. Phys. 20, 1813 (1952); Jenckel, E. and H. Rinkens, Z. Elektrochem. 60, 970 (1956); and Fortune, L. R. and G. N. Malcolm, J. Phys. Chem. 64, 934 (1948).
16. Bridgman, P. W., Proc. Am. Acad. Arts. Sci. 76, 71 (1948).
17. Parks, W. and R. B. Richards, Trans. Faraday Soc. 45, 203 (1949).
18. Matsuoka, S., J. Polymer Sci. 42, 511 (1960).
19. Lupton, J. M., Trans. SPE 1, 105 (1961).
20. Hellwege, K. H., W. Knappe and P. Lehmann, Kolloid Z. 183, 110 (1962).
21. Matsuoka, S., J. Polymer Sci. 57, 569 (1962).
22. Wunderlich, B. Rev. Sci. Instr. 32, 1424 (1961).
23. Bridgman, P. W., The Physics of High Pressure, G. Bell and Sons, London, 1949.
24. Comings, E. W., High Pressure Technology, McGraw Hill Book Company, New York, 1956.
25. Wunderlich, B. and D. Poland, J. Polymer Sci. A-1, 357 (1963).
26. Bodily, D., Ph.D. Thesis, Cornell University, Ithaca, New York, 1964.
27. Swan, P. R., J. Polymer Sci. 56, 403 (1962).

28. Gubler, M. G. and A. J. Kovacs, J. Polymer Sci. 34, 551 (1959).
29. Nielsen, L. E., J. Appl. Phys. 25, 1209 (1954).
30. Bekkedahl, N., J. Res. Natl. Bur. Std. 43, 145 (1949).
31. Marker, L., R. Early and S. L. Aggarwal, J. Polymer Sci. 38, 369 (1959).
32. Richardson, M. J., P. J. Flory and J. B. Jackson, Polymer 4, 221 (1963).
33. Cole, E. A. and D. R. Holmes, J. Polymer Sci. 46, 245 (1960).
34. Hendus, H. and G. Schnell, Kunststoffe 51, 69 (1961).
35. Wunderlich, B. and M. Dole, J. Polymer Sci. 24, 201 (1957).
36. Maley, L. E., Paper presented at Am. Chem. Soc. Meeting, Chicago, Illinois, September, 1964.
37. Bunn, C. W., A. J. Cobbold and R. P. Palmer, J. Polymer Sci. 28, 365 (1958).
38. Speerschneider, C. J. and C. H. Li, J. Appl. Phys. 33, 1871 (1962).
39. Geil, P. H., F. R. Anderson, B. Wunderlich and T. Arakawa, J. Polymer Sci. A-2, 3707 (1964).
40. Anderson, F. R., J. Appl. Phys. 35, 64 (1964).
41. Anderson, F. R., J. Polymer Sci. C-3, 123 (1963).
42. Statton, W. O. and P. H. Geil, J. Appl. Polymer Sci. 3, 357 (1960).

43. Fischer, E. W. and G. F. Schmidt, *Angew. Chem.* 74, 551 (1962).
44. Geil, P. H., *Bull. Am. Phys. Soc.* 7, 206 (1962).
45. Speerschneider, C. J. and C. H. Li, *J. Appl. Phys.* 34, 3004 (1963).
46. Kratky, O. and G. Porod, *J. Colloid Sci.* 4, 35 (1949).
47. Dexter, D. J., *Phys. Rev.* 90, 1007 (1953).
48. Flory, P. J., *J. Am. Chem. Soc.* 84, 2857 (1962).
49. Kabalkina, S. S. and Z. V. Troitskaya, *J. Structural Chem.* 2, 22 (1961).
50. Müller, A., *Proc. Roy. Soc.* A-178, 227 (1941).
51. Bunn, C. W., *Trans. Faraday Soc.* 35, 482 (1939).
52. Pierce, R. H., J. P. Tordella and W. M. D. Bryant, *J. Am. Chem. Soc.* 74, 282 (1952).
53. Slichter, W. P., *J. Polymer Sci.* 21, 141 (1956).
54. Teare, P. W. and D. R. Holmes, *J. Polymer Sci.* 24, 496 (1957).
55. Turner Jones, A., *J. Polymer Sci.* 62, S 53 (1962).
56. Tanaka, K., T. Seto and T. Hara, *J. Phys. Soc. Japan* 17, 873 (1962).
57. Powers, J. and A. Van Valkenburg, *Bull. Am. Phys. Soc.* 8, 243 (1963).
58. Vonk, C. G., *Nature (London)* 186, 962 (1960).
59. Hermans, P. H. and A. Weidinger, *Makromol. Chem.* 44, 24 (1962).

60. Westover, R. F., Trans. SPE 1, 14 (1961).
61. Steele, W. A. and W. Webb in High Pressure Physics and Chemistry (Ed. R. S. Bradley), Academic Press, New York, 1963.
62. Turnbull, D. and J. C. Fisher, J. Chem. Phys. 17, 71 (1949).
63. Wunderlich, B. and T. Arakawa, J. Polymer Sci. A-2, 3697 (1964).
64. Wunderlich, B., J. Polymer Sci. A-1, 1245 (1963).
65. Brown, R. G. and R. K. Eby, J. Appl. Phys. 35, 1156 (1964).
66. Matsuoka, S., J. Appl. Polymer Sci. 4, 115 (1960).
67. Mandelkern, L., Crystallization of Polymers, McGraw-Hill Book Company, New York, 1964.
68. Mandelkern, L., M. Hellmann, D. W. Brown, D. E. Roberts and F. A. Quinn, Jr., J. Am. Chem. Soc. 75, 4093 (1953).
69. Matsuoka, S. and C. J. Aloisio, Bull. Am. Phys. Soc. 8, 243 (1963).
70. Wunderlich, B., J. Chem. Phys. 29, 1395 (1958).
71. Wunderlich, B., to be published.
72. Wunderlich, B. and W. H. Kashdan, J. Polymer Sci. 50, 71 (1961).
73. Wunderlich, B., P. Sullivan, T. Arakawa, A. B. DiCyan and J. F. Flood, J. Polymer Sci. A-1, 3581 (1963).

74. Wunderlich, B., Polymer 5, 125 (1964).
75. Bodily, D. and B. Wunderlich, to be published.
76. Wunderlich, B., E. Hellmuth and H. Bauer, Paper presented at Am. Chem. Soc. Meeting, Chicago, Illinois, 1964.
77. Day, A. L. and E. T. Allen, Carnegie Inst. Wash. Publ. 31 (1905).
78. Doelter, C., Z. Elektrochem. 12, 413 (1906).
79. Volmer, M. and O. Schmidt, Z. physik. Chem. B-35, 467 (1937).
80. Greig, J. W. and T. F. W. Barth, Am. J. Sci. A-35, 93 (1938).
81. Khaikin, S. E. and N. P. Bene, Compt. rend. acad. Sci., U.S.S.R. 23, 31 (1939).
82. Sears, G. W., J. Phys. Chem. Solids 2, 37 (1957).
83. Ainslie, N. G., J. D. Mackenzie and D. Turnbull, J. Phys. Chem. 65, 1718 (1961).
84. Cormia, R. L., J. D. Mackenzie and D. Turnbull, J. Appl. Phys. 34, 2239 (1963).
85. Eiermann, K., J. Polymer Sci. C-6, 157 (1964).
86. Tammann, G., The State of Aggregation, D. Van Nostrand Company, New York, 1925.
87. Chiang, R. and P. J. Flory, J. Am. Chem. Soc. 83, 2857 (1961).
88. Broadhurst, M. G., J. Chem. Phys. 36, 2578 (1962); J. Res. Natl. Bur. Std. A-66, 241 (1962).

89. Flory, P. J. and A. Vrij, J. Am. Chem. Soc. 85, 3548 (1963).
90. Hoffman, J. D. and J. J. Weeks, J. Res. Natl. Bur. Std. A-66, 13 (1962).
91. Bryant, W. M. D., J. Polymer Sci. 34, 595 (1959).
92. Willbourn, A. J., J. Polymer Sci. 34, 569 (1959).
93. Flory, P. J., J. Chem. Phys. 17, 223 (1949).
94. Flory, P. J., Trans. Faraday Soc. 51, 848 (1955).
95. Walter, E. R. and F. P. Reding, J. Polymer Sci. 21, 561 (1956).
96. Eichhorn, R. M., J. Polymer Sci. 31, 197 (1958).
97. Swan, P. R., J. Polymer Sci. 56, 409 (1962).